

WEATHER RADAR DATA ASSIMILATION IN THE ALADIN-HIRLAM NWP SHARED SYSTEM

EXPERIMENTS AND DEVELOPMENTS DONE AT
AEMET

CARLOS GEIJO

38th EWGLAM-23rd SRNWP EUMETNET Meeting. Rome October 2016

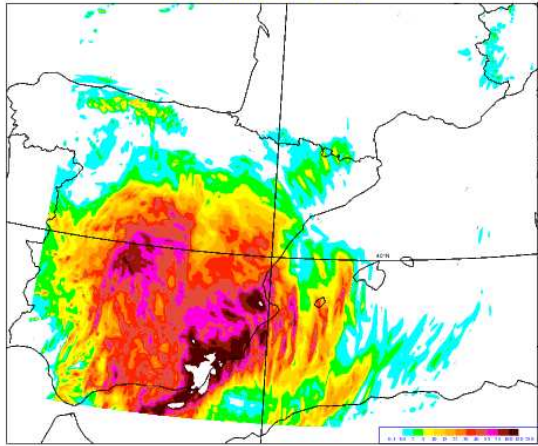
Some Milestones in the last Years in Radar Data Assimilation in HIRLAM-AEMET

- Kick-off HIRLAM working week in Oslo with participation of Météo-France (March 2010)
- Sep 2011, Release of CONRAD Software (Converter of Radar Local Format to Météo-France DIM in BUFR). Adaptation to AEMET DIM in BUFR and first tests with ALADIN-3DVar (HARMONIE v36) (Nov 2011).
- Tests of Z assimilation in HARMONIE-AEMET with a first Field Alignment Prototype (April 2012)
- Collaboration with Météo-France in HyMex-SOP1 (Sep-Nov 2012). Impact Studies with AROME-WMED and SOP-1 Data (June 2013)
- Tests of DOW assimilation in HARMONIE-AEMET using the Field Alignment method and SOP-1 Data (April 2013). Communication at the 6th WMO Symposium on DA (October 2013)
- Installation (Autumn 2013) of BALTRAD QC Toolbox and tests in NRT (2013-2014)
- Tests with Z and DOW simulated observations in AEMET-HARMONIE using the Field Alignment method (April 2014)
38th EWGLAM-23rd SRNWP EUMETNET Meeting. Rome October 2016
- Release of the Field Alignment Software for HARMONIE v38 (April 2015)

Météo-France IMPACT STUDY WITH AROME-WMED, SOI

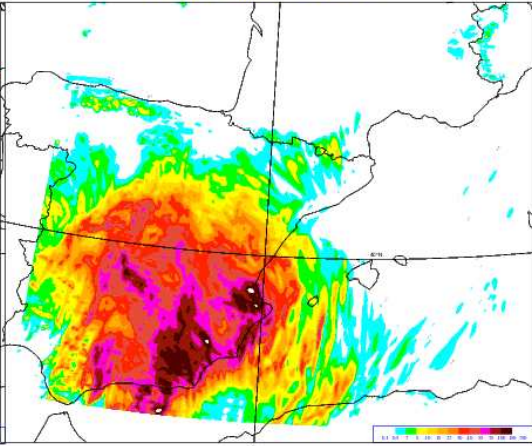
2012092800 7AHL / RR P24-P00

ICMSHAROM+0024 - 0 field: PRECIP -



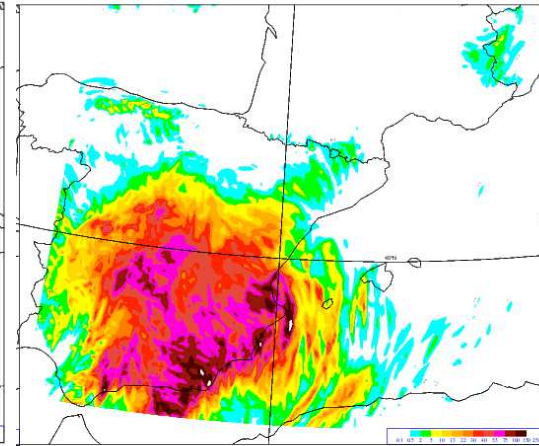
2012092800 7AKN / RR P24-P00

ICMSHAROM+0024 - 0 field: PRECIP -



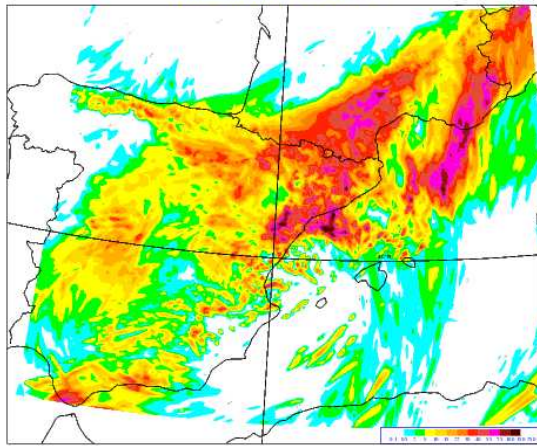
2012092800 7AZV / RR P24-P00

ICMSHAROM+0024 - 0 field: PRECIP -



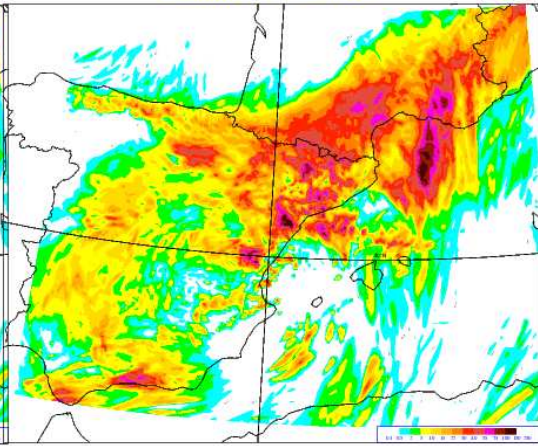
2012092900 7AHL / RR P24-P00

ICMSHAROM+0024 - 0 field: PRECIP -



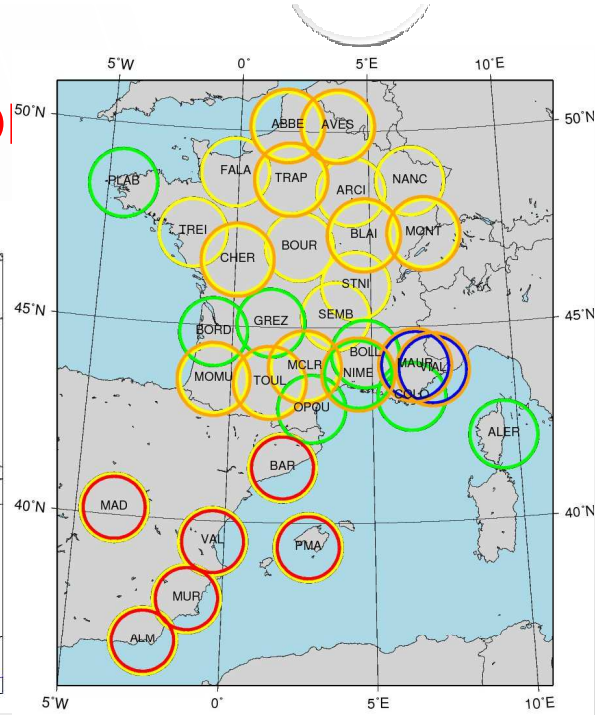
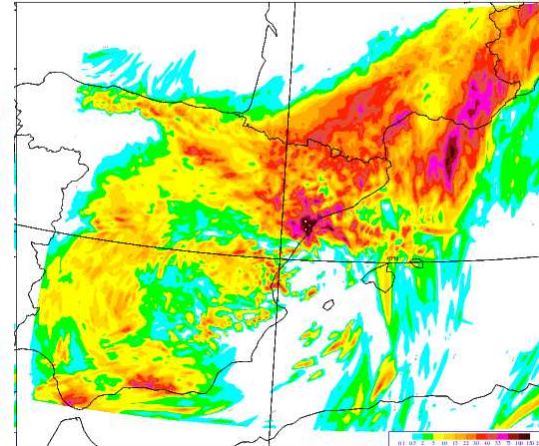
2012092900 7AKN / RR P24-P00

ICMSHAROM+0024 - 0 field: PRECIP -



2012092900 7AZV / RR P24-P00

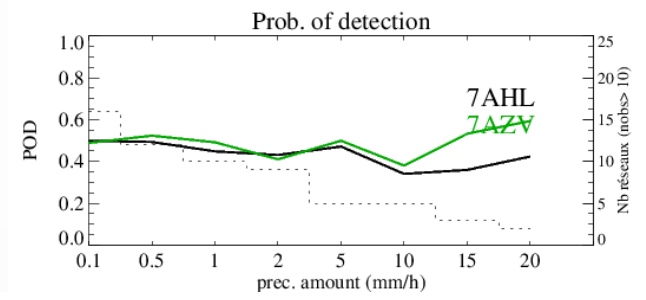
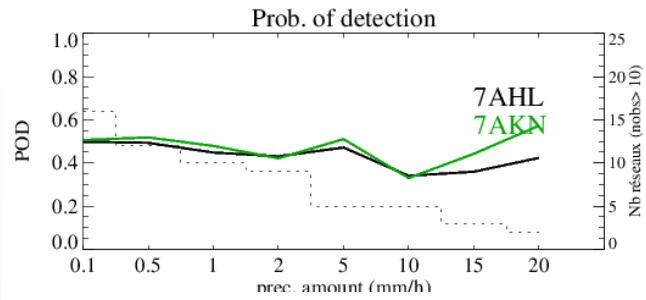
ICMSHAROM+0024 - 0 field: PRECIP -



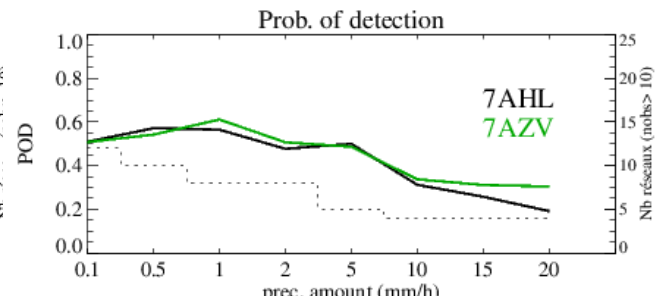
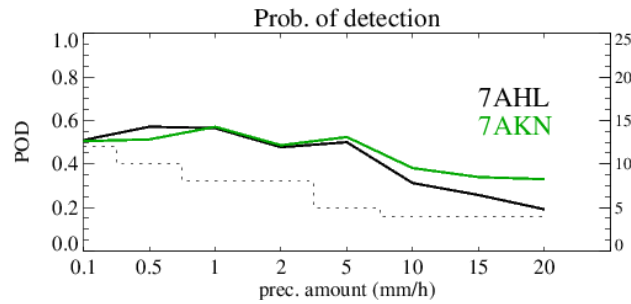
7AHL : CNTRL: Arome WMED
7AKN : EXP 6 radars AEMET en plus
7AZV : 7AKN sans les Z AEMET

POD
27/09 -> 8/10

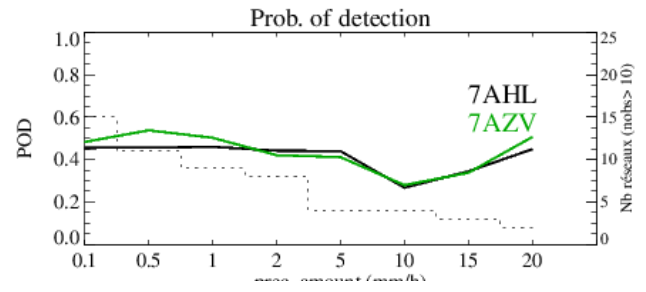
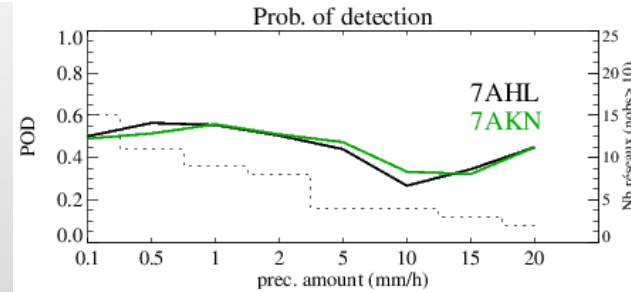
RR6 P0->P6



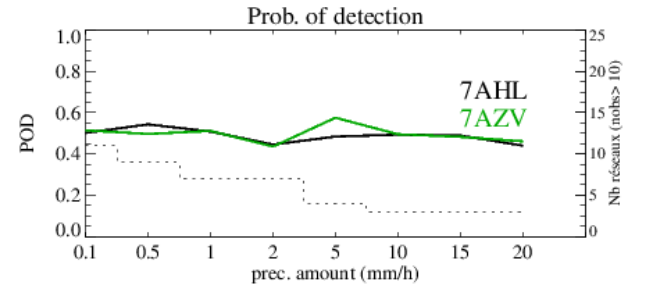
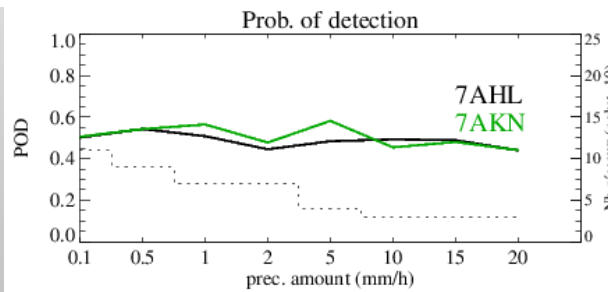
RR6 P6->P12



RR6 P12->P18

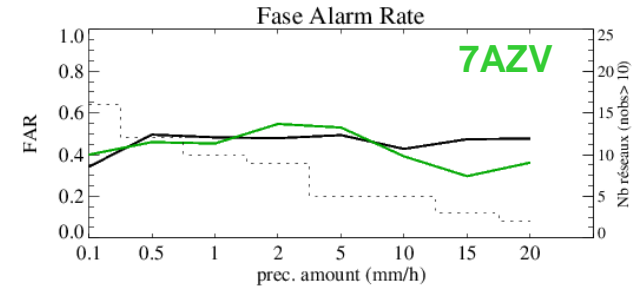
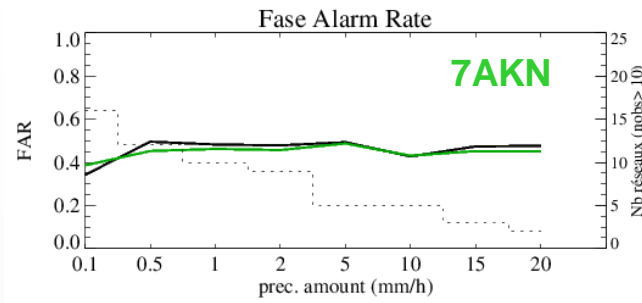


RR6 P18->P24

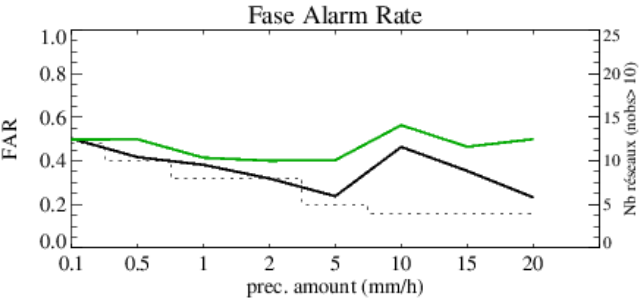
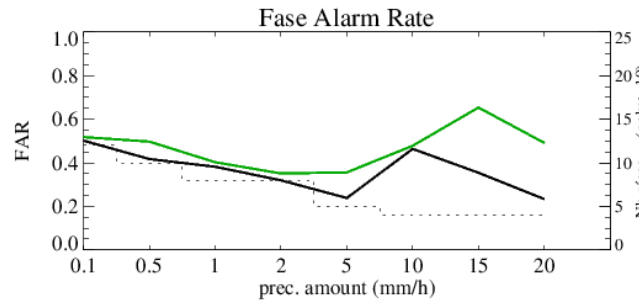


FAR
27/09 -> 8/10

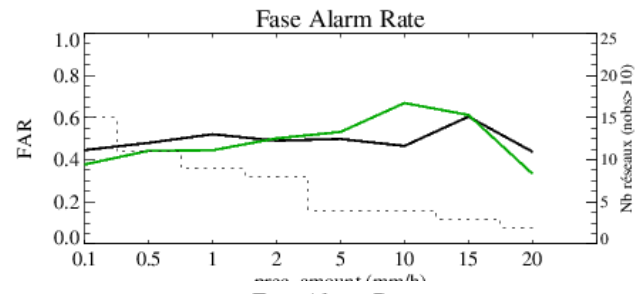
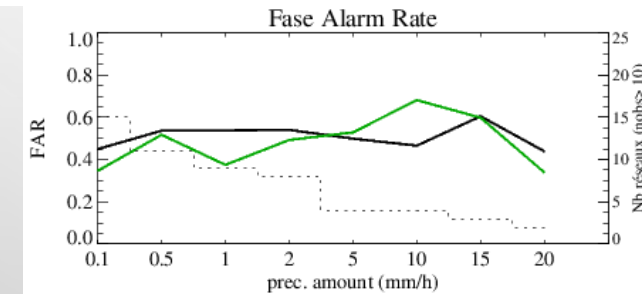
RR6 P0->P6



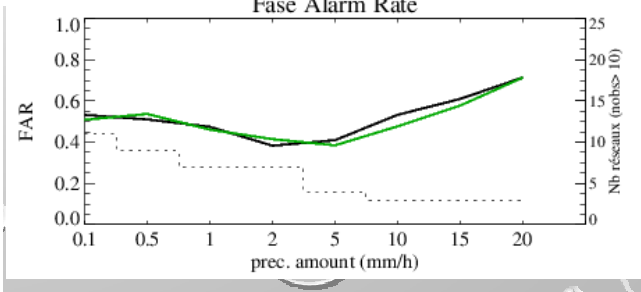
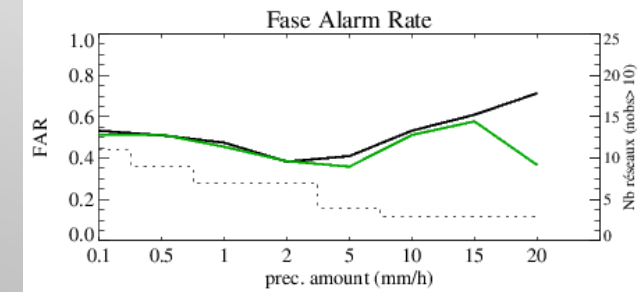
RR6 P6->P12



RR6 P12->P18

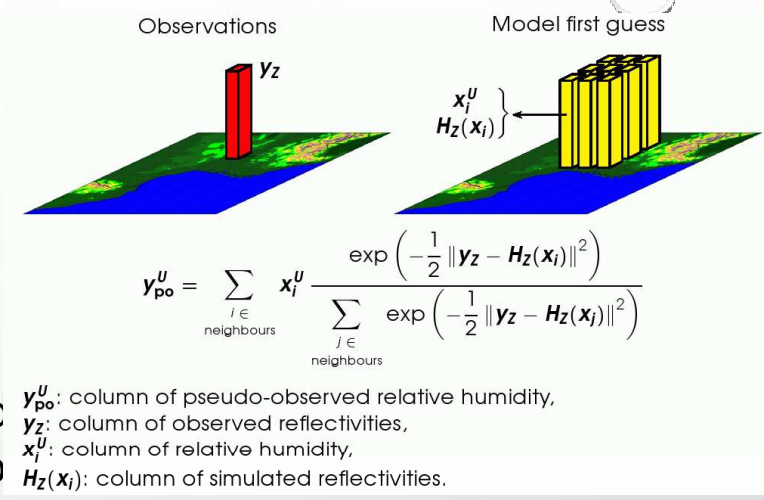


RR6 P18->P24



A NEW METHOD FOR ASSIMILATION OF WEATHER RADAR DATA: FIELD ALIGNMENT

- In the 1D-3DVar method for Z assimilation (Caumont et al, 2010) model profiles in the neighbourhood of the observation location are used to construct a likelihood $P(y|x)$ for the observed profiles. "it is expected [...] the model [...] similar to what is observed, but at the wrong location"
- In the Field Alignment method (Ravela et al, 2007), the likelihood constructed from a displaced model state. The method explicitly represents position errors by introducing in the analysis control space a displacement vector field q , defined in each analysis grid point, that gives the deformation necessary to minimize these position errors



$$P(X, q | Y) \propto P(Y | X, q)$$

"data likelihood".
 Connects observations to the displaced model state

$$P(X^f | q)$$

"amplitude prior".
 Says that the forecast statistics are conditioned on the displacement field q (e.g. $B(q)$)

$$P(q)$$

"displacement prior"
 enables the introduction of smoothness constraints on the q field

In the usual assumptions of gaussianity for these component PDF problem is casted into that of minimization of a cost function

$$2J_{FA} = \left(X(\vec{p}) - X^f(\vec{p}) \right)^T B(\vec{q})^{-1} \left(X(\vec{p}) - X^f(\vec{p}) \right) + \frac{\partial J}{\partial X} = 0 \quad (1) \quad ; \quad \frac{\partial J}{\partial \vec{q}} = 0 \quad (2)$$

$$\left(Y - H X(\vec{p}) \right)^T R^{-1} \left(Y - H X(\vec{p}) \right) + 2L(\vec{q}) - \ln(|B(\vec{q})|)$$

where $X(\mathbf{p} = \mathbf{r} - \mathbf{q})$ represents X displaced by \mathbf{q}

In the “sequential algorithm” to solve this complex problem, (2) is just the alignment equation :

$$w_1 \Delta \vec{q} + w_2 \nabla \left(\nabla \cdot \vec{q} \right) = \left(\nabla X^f \Big|_{\vec{p}} \right)^T H^T R^{-1} \left(Y - H X^f(\vec{p}) \right)$$

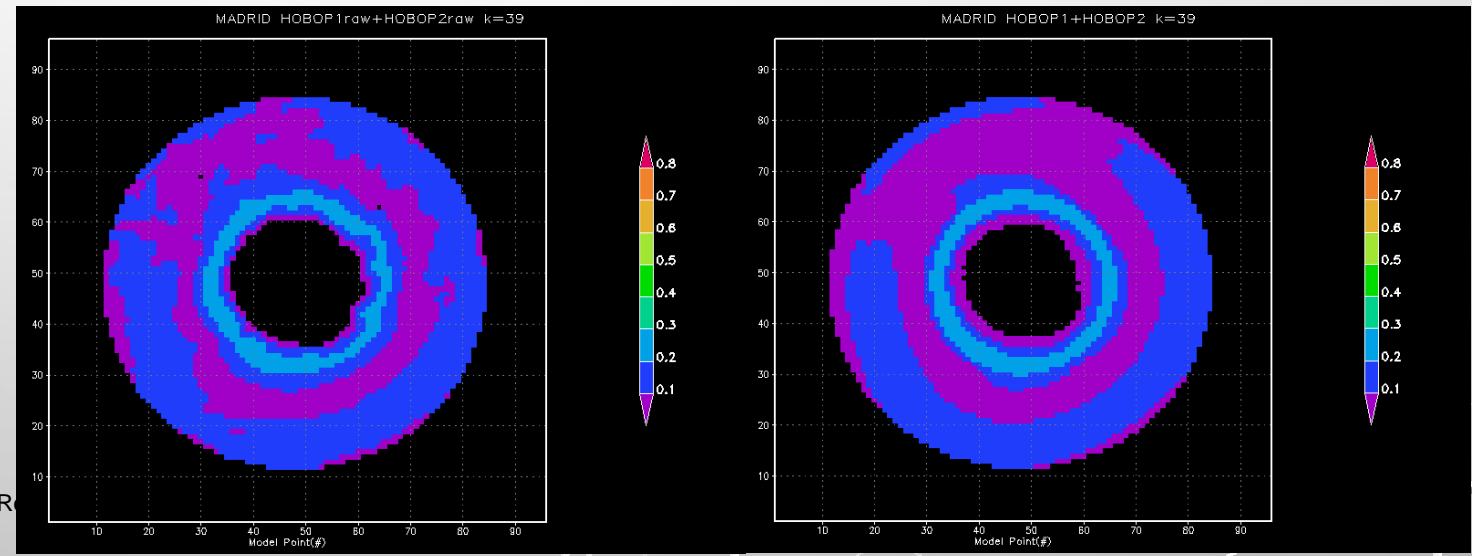
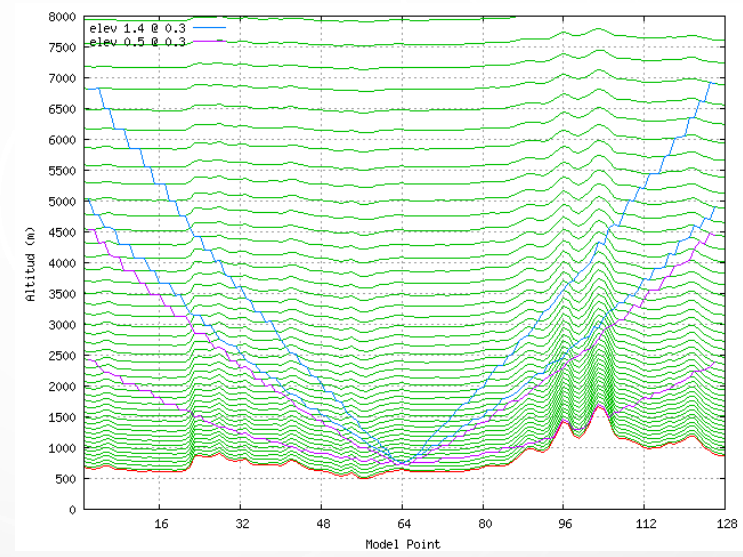
Calculation of the Obs Operator

$$w_1 \Delta \vec{q} + w_2 \nabla (\nabla \cdot \vec{q}) + (\nabla X^f)^T \mathbf{H}^T \mathbf{R}^{-1} (\mathbf{H} X^f - Y) = 0$$

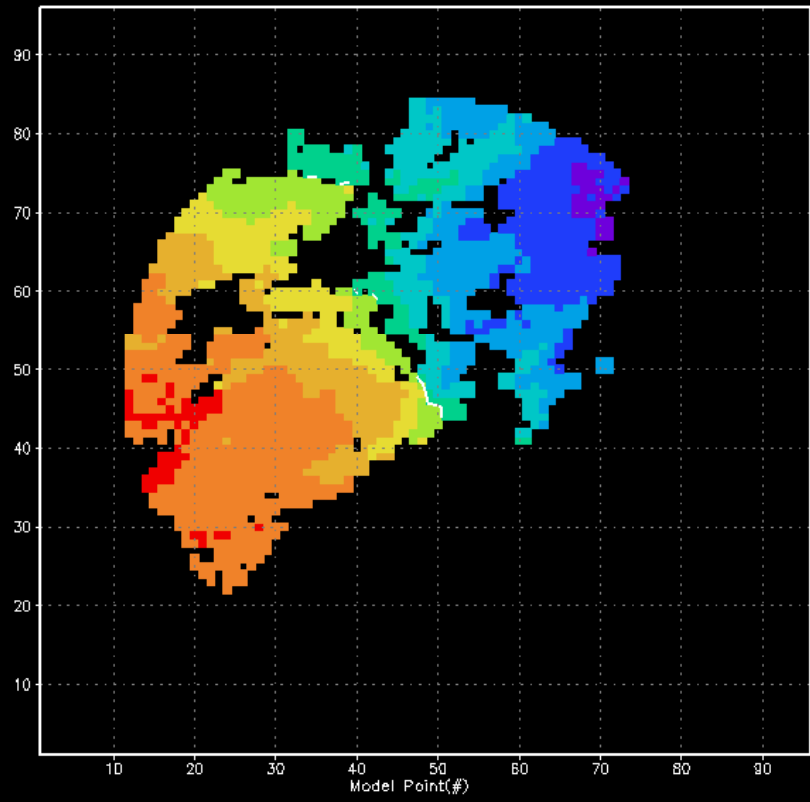
$$H = H(i, j, lev, PPI); \sum_{lev} H(i, j, lev, PPI) = 1;$$

$$HX = \sum_{lev} H(i, j, lev, PPI) X(i, j, lev)$$

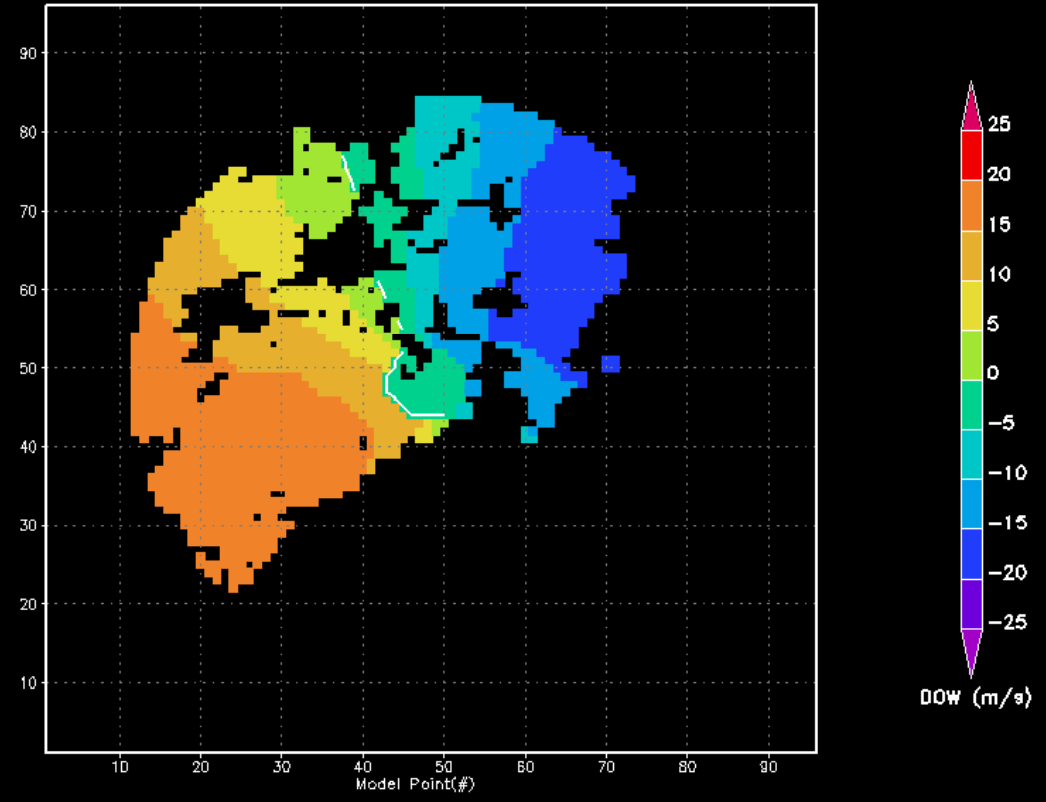
$$H^T X = \sum_{PPI} H(i, j, lev, PPI) X(i, j, PPI)$$



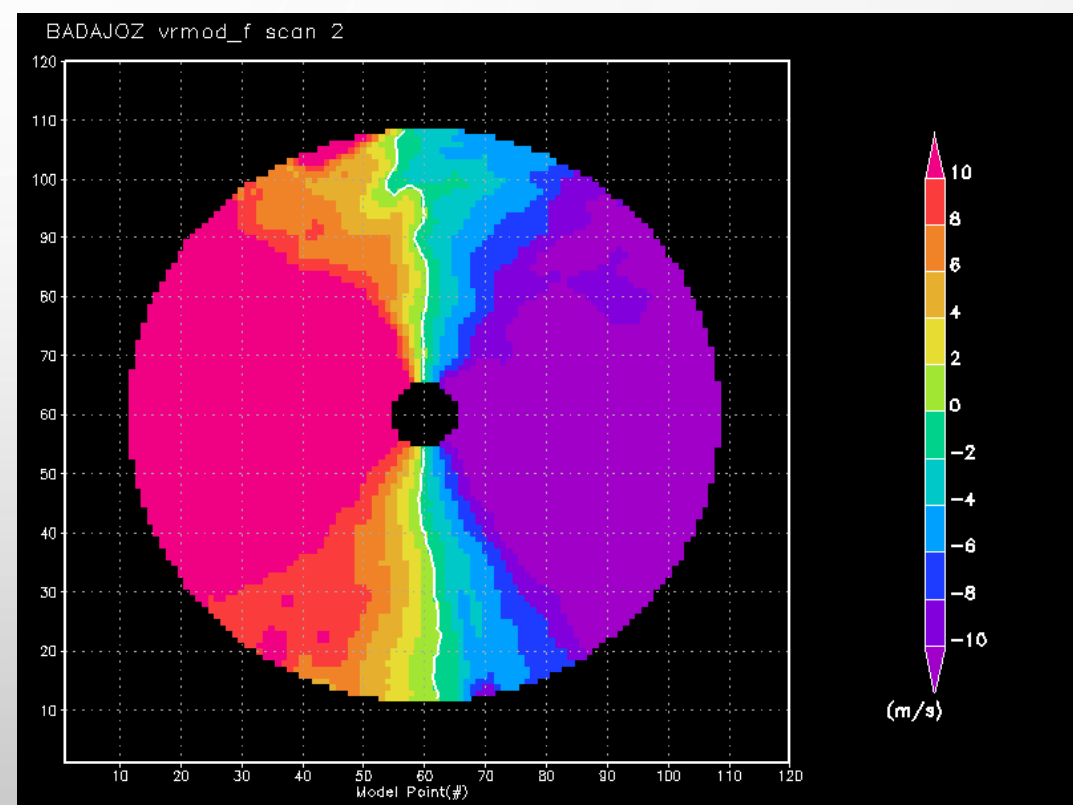
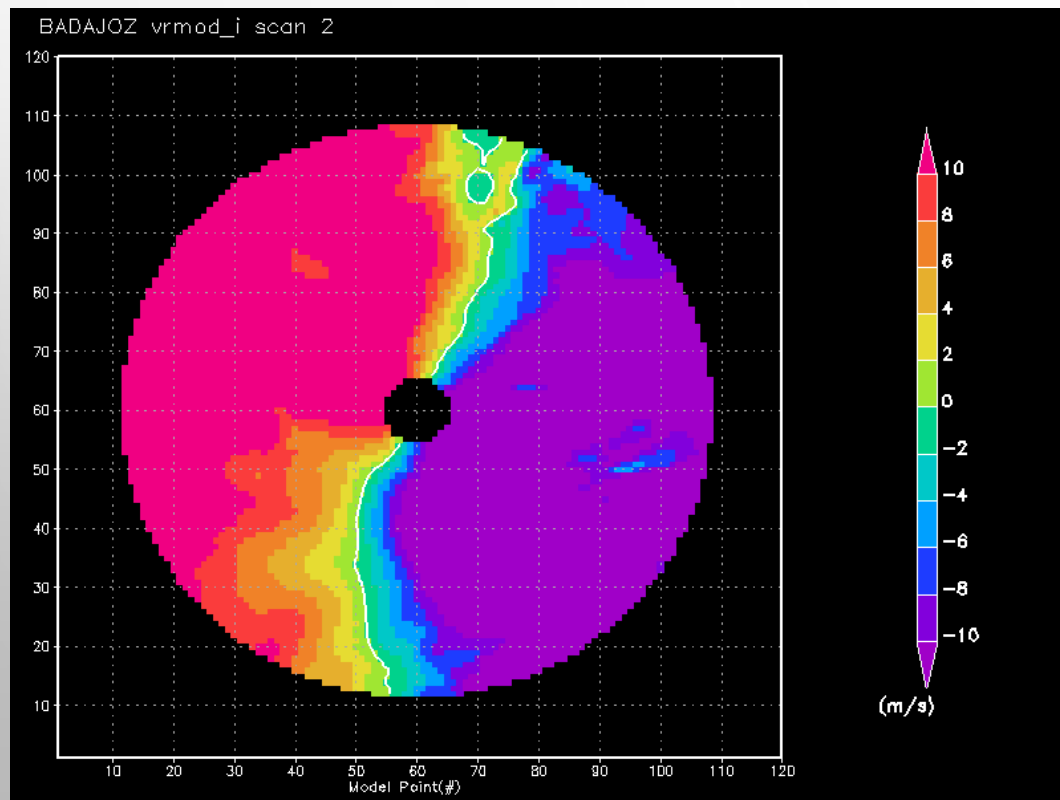
Blended fc_start 2012092600 ; obsscan2 iter 1 (WND)

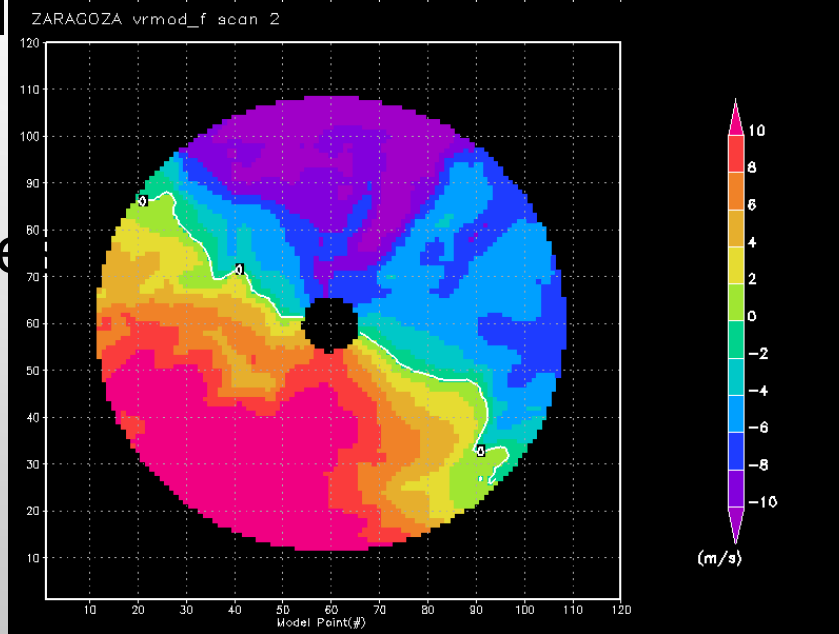
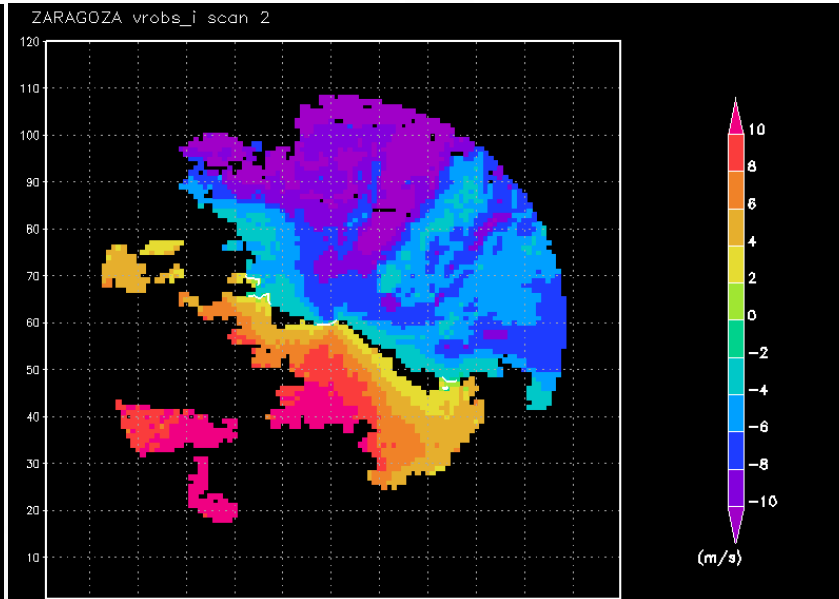
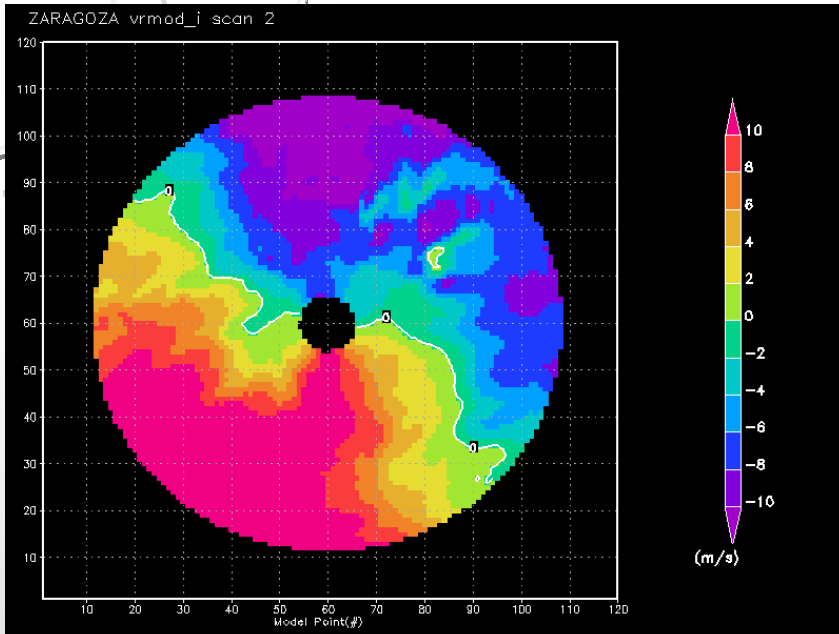


Blended fc_start 2012092600 ; mskmodscan2 iter 46 (WND)



the FA method is indeed able to extract a lot of information from the radar DC observations, here for example the whole wind field is rotated





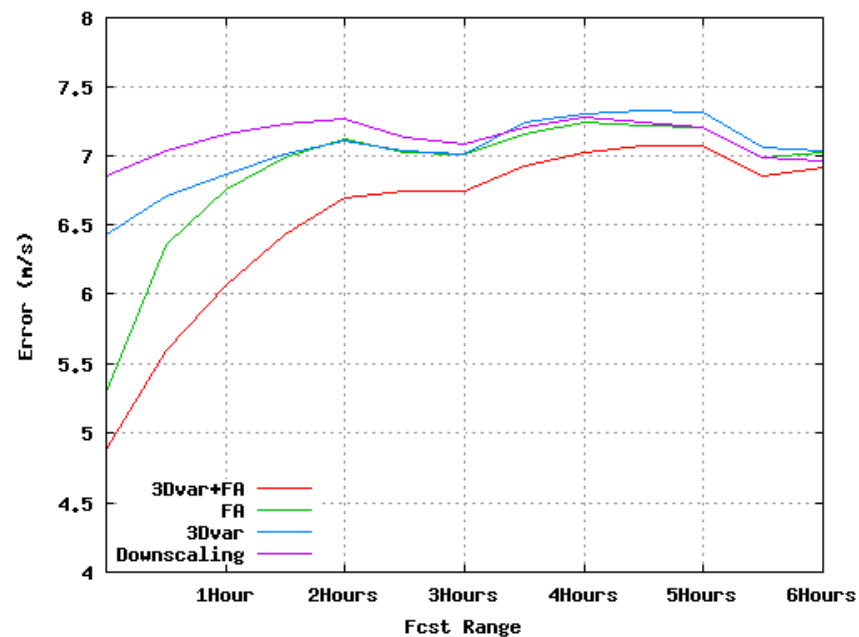
... or to pick up convergence line

Assimilation of Doppler Wind Radar Data in HARMONIE

- Verification of forecasted radial wind using the own radar data:

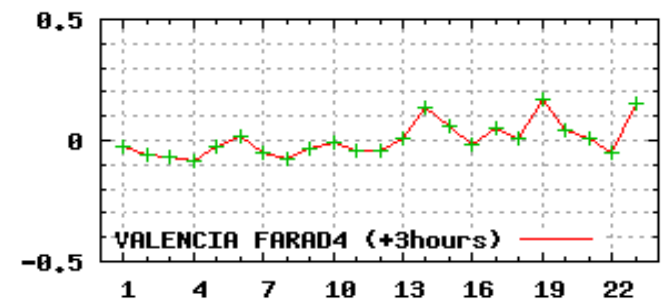
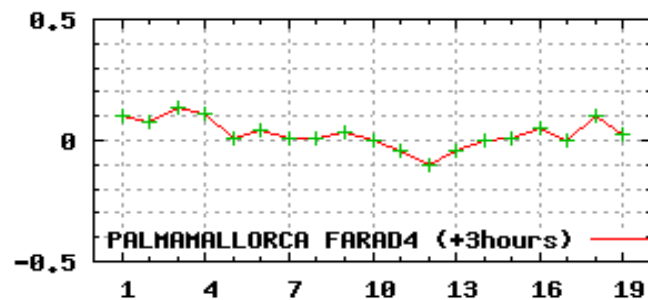
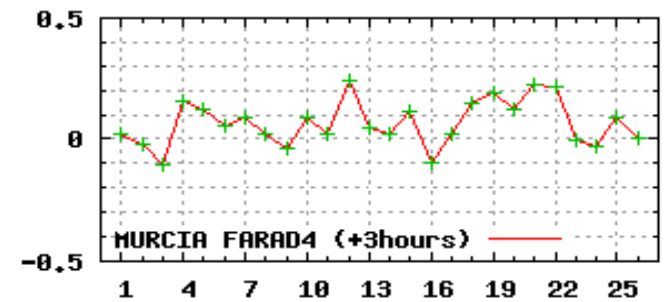
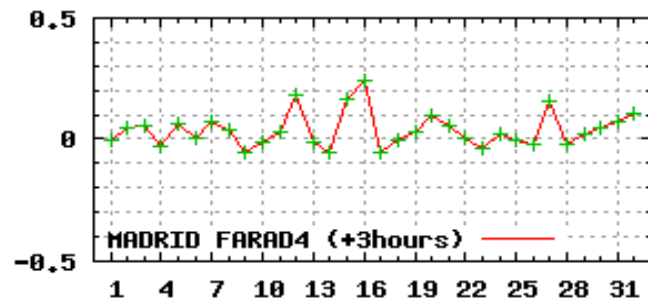
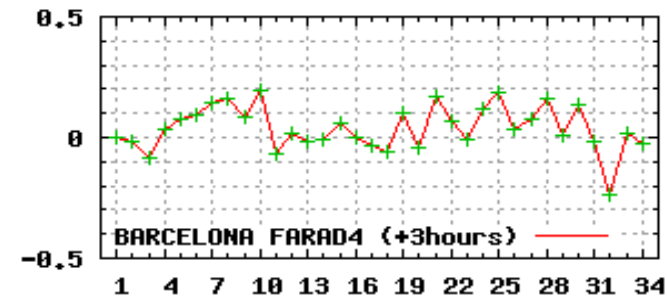
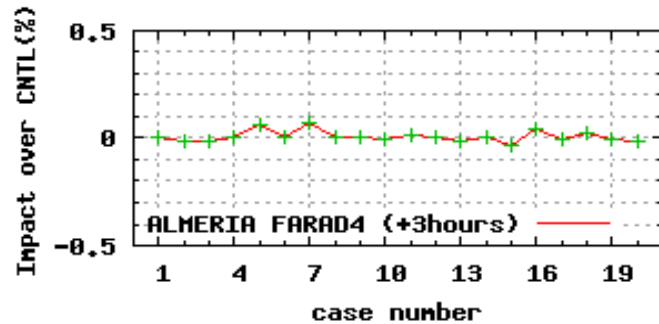
$$\text{Error} \equiv \left\langle (\text{Fcst} - \text{Radar})^2 \right\rangle_{\text{PPI}=0.5}^{1/2} + \left\langle (\text{Fcst} - \text{Radar})^2 \right\rangle_{\text{PPI}=1.4}^{1/2}$$

- Results averaged over more than 150 cases (HyMex SOP-1):



Assimilation of Doppler Wind Radar Data in HARMONIE

- Case-by-case analysis of the Impact (+3Hours) (SOP-1 data):



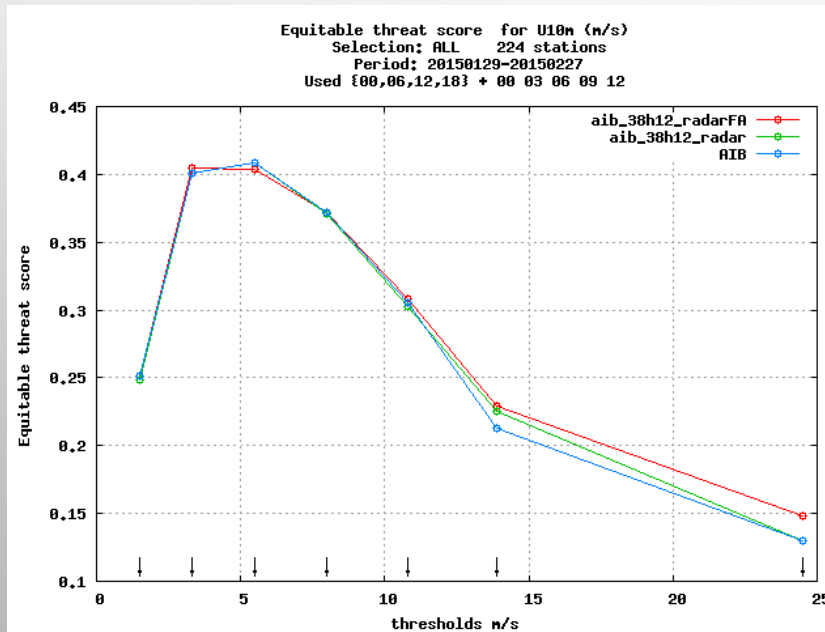
Operational Verification

Sample Size: 222 stations, 1 month (Feb 2015)

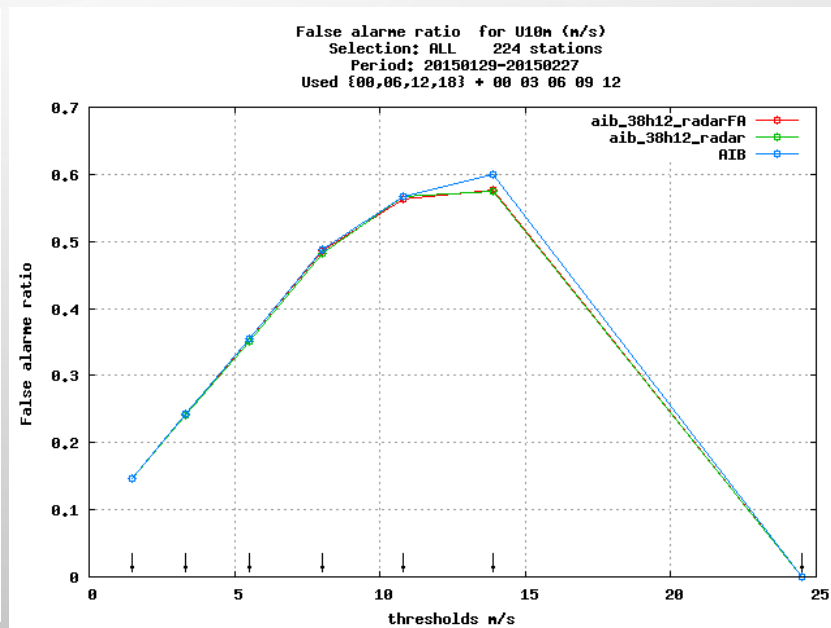
Parameter : 10m wind speed

Settings : FCST up to +12H, 3H cycle DA (Z and DOW assimilation)

Equitable Threat Score



False Alarm Ratio



Operational Verification

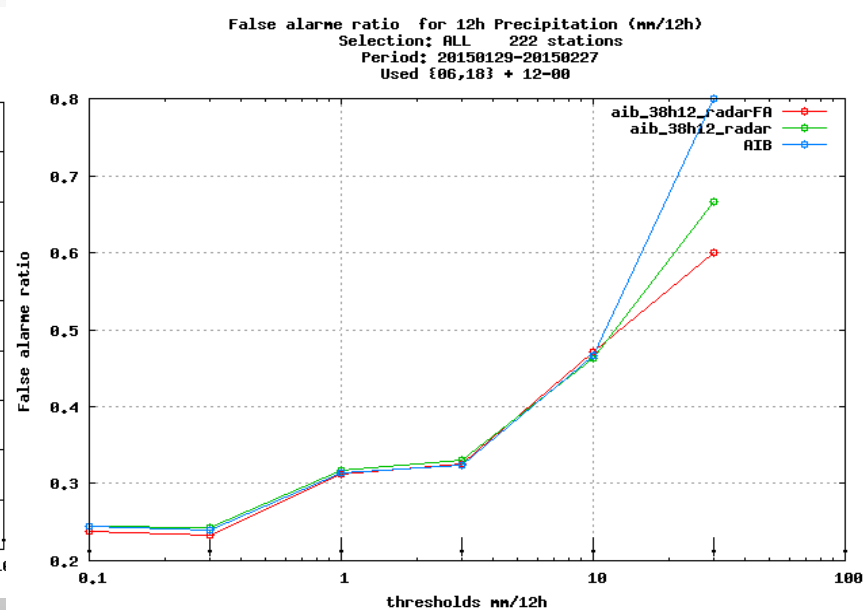
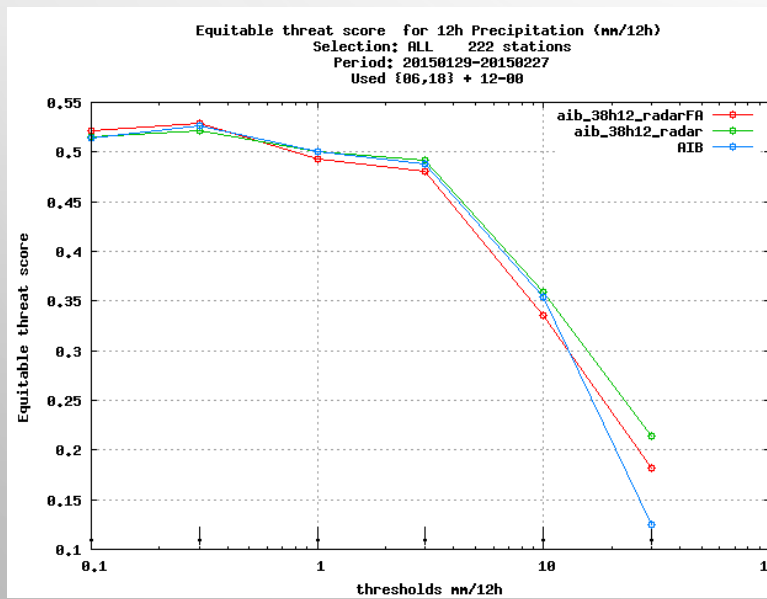
Sample Size: 222 stations, 1 month (Feb 2015)

Parameter : Precipitation (mm/12H)

Settings : FCST up to +12H, 3H cycle DA (Z and DOW assimilation)

EquitableThreat Score

False Alarm Ratio



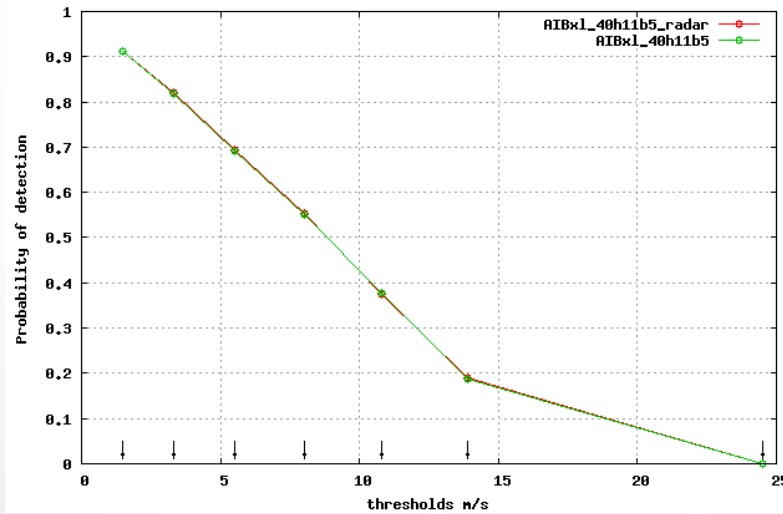
10m wind

Operational Verification

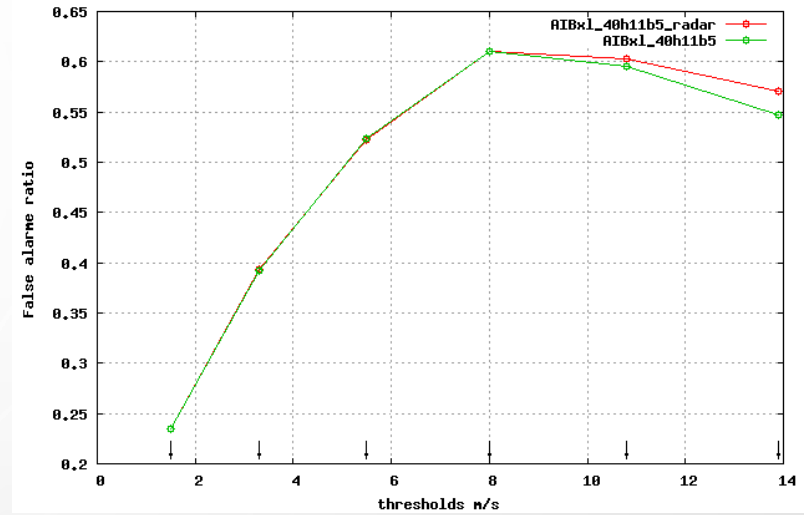
Sample size :
844 stations,
1 month (April 2016)

Settings :
up to +12H FCST,
3H cycle DA
Just DOW
assimilation

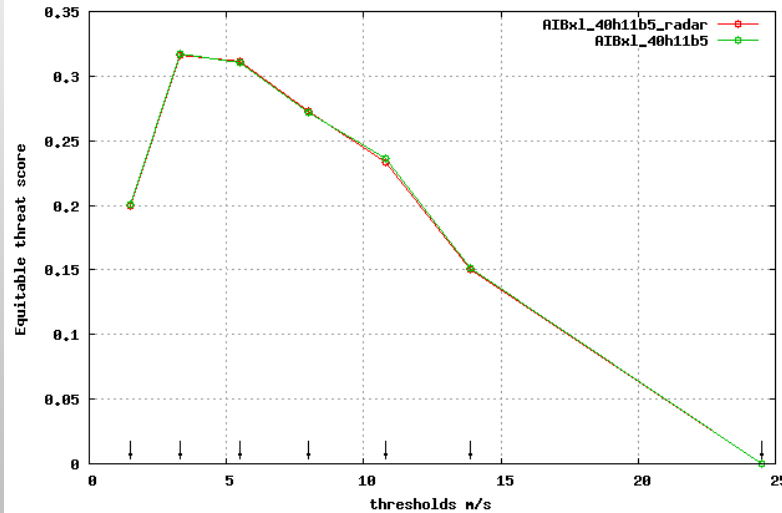
Probability of detection for U10m (m/s)
Selection: ALL 844 stations
Period: 20160401-20160430
Used {00,03,...,21} + 03 06 09 12



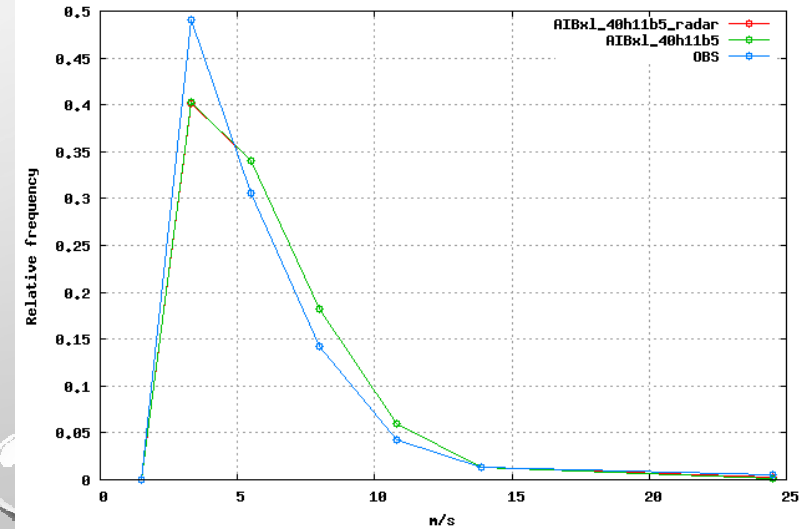
False alarm ratio for U10m (m/s)
Selection: ALL 844 stations
Period: 20160401-20160430
Used {00,03,...,21} + 03 06 09 12



Equitable threat score for U10m (m/s)
Selection: ALL 844 stations
Period: 20160401-20160430
Used {00,03,...,21} + 03 06 09 12



Selection: ALL 844 stations
U10m Period: 20160401-20160430
Used {00,03,...,21} + 03 06 09 12



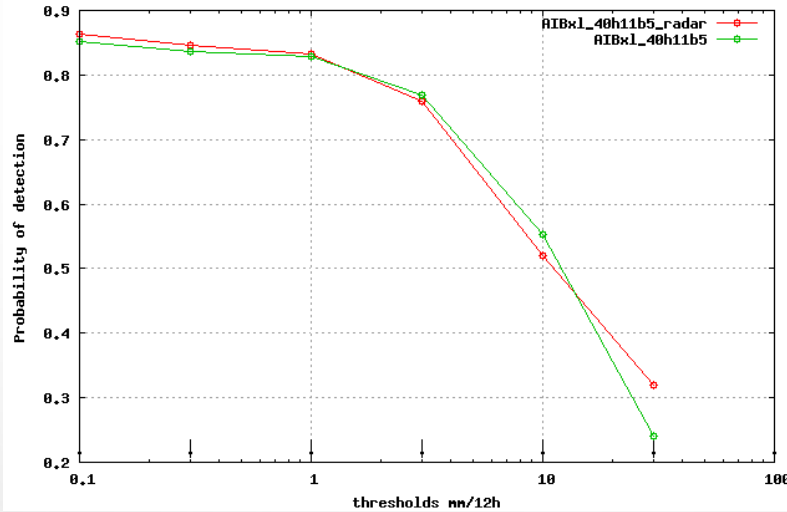
12 hours Precipitation

Operational Verification

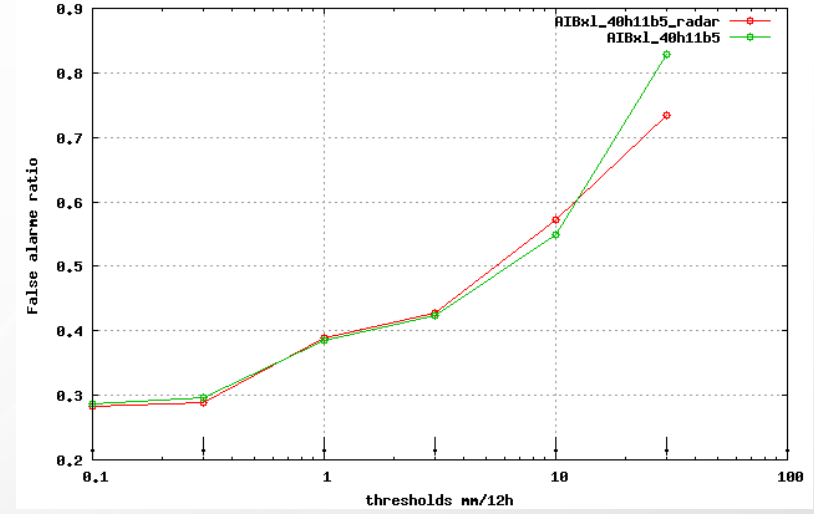
Sample size :
844 stations,
1 month (April 2016)

Settings :
up to +12H FCST,
3H cycle DA
Just DOW
assimilation

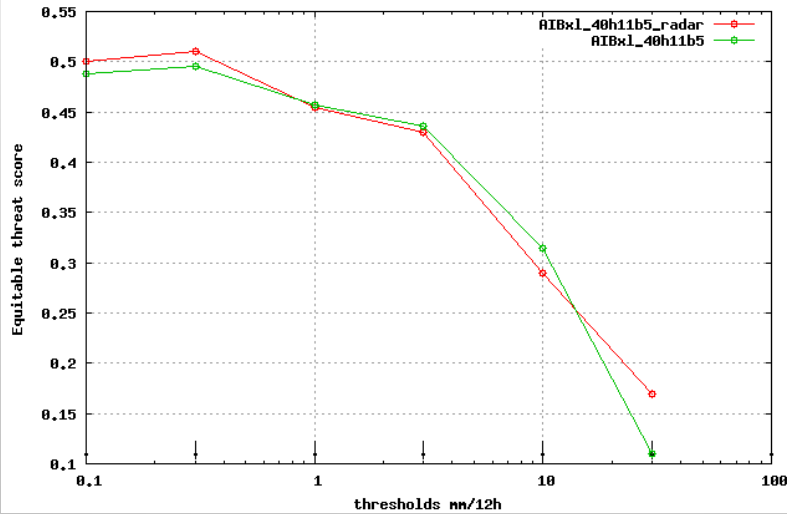
Probability of detection for 12h Precipitation (mm/12h)
Selection: ALL 469 stations
Period: 20160401-20160430
Used {06,18} + 12-00



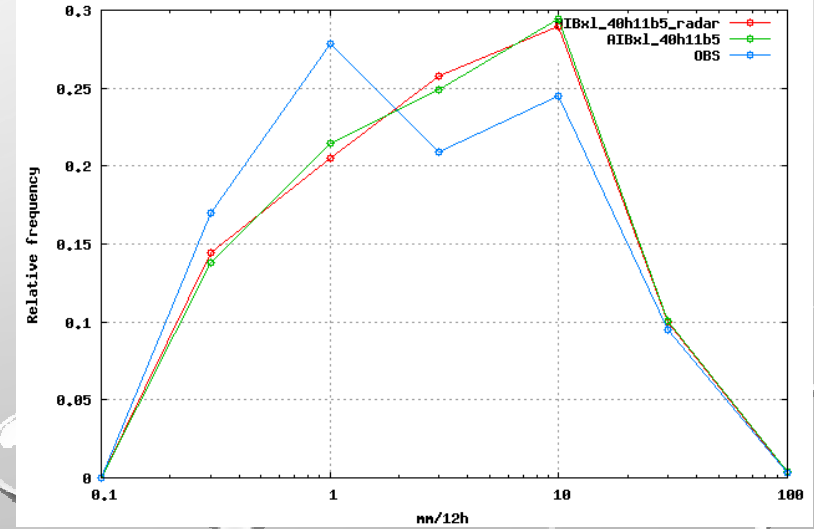
False alarm ratio for 12h Precipitation (mm/12h)
Selection: ALL 469 stations
Period: 20160401-20160430
Used {06,18} + 12-00



Equitable threat score for 12h Precipitation (mm/12h)
Selection: ALL 469 stations
Period: 20160401-20160430
Used {06,18} + 12-00



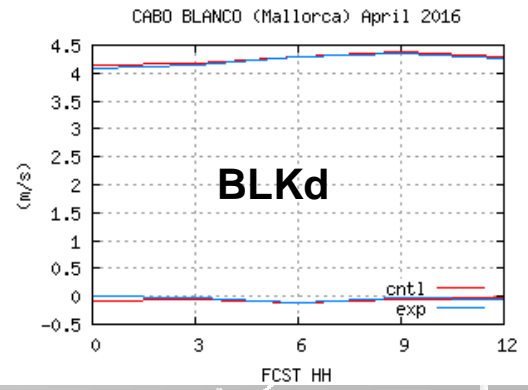
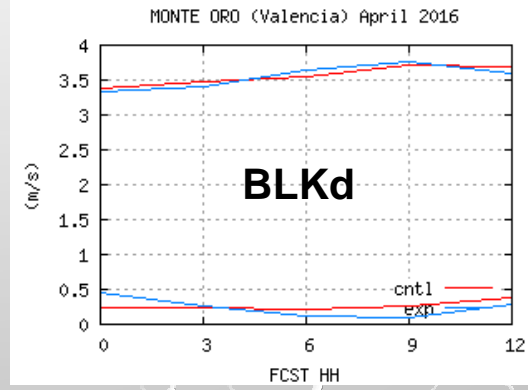
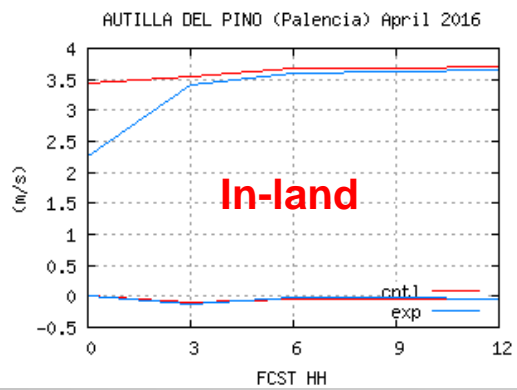
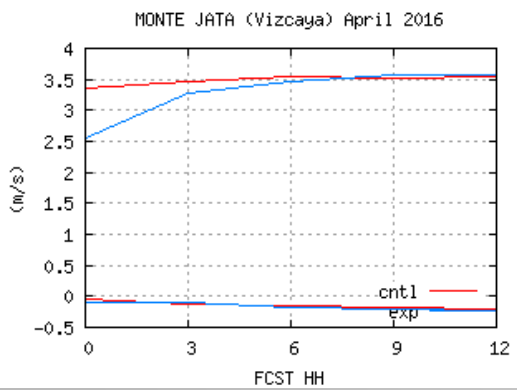
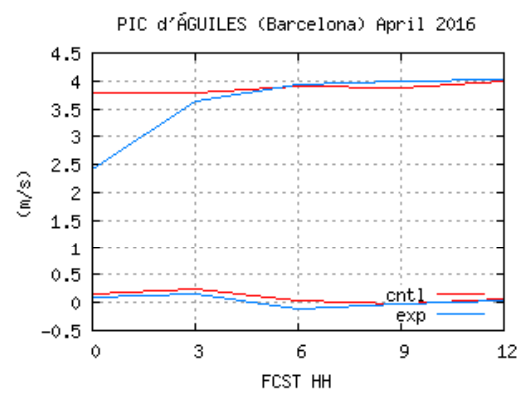
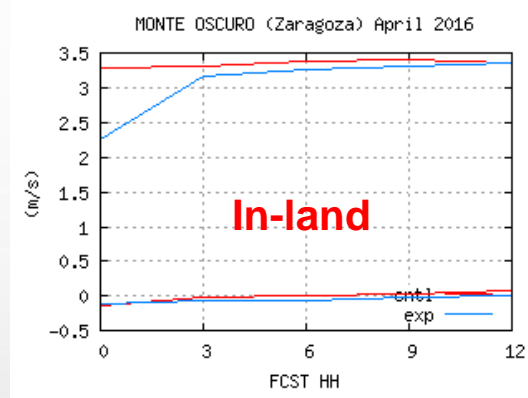
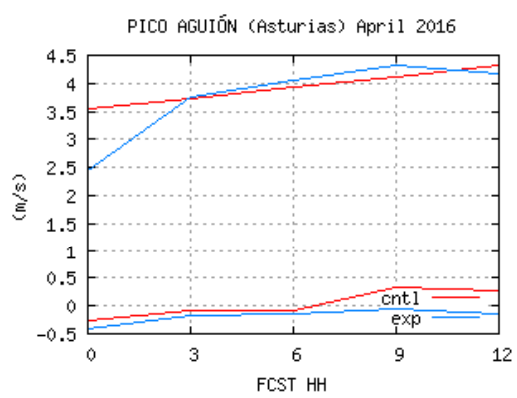
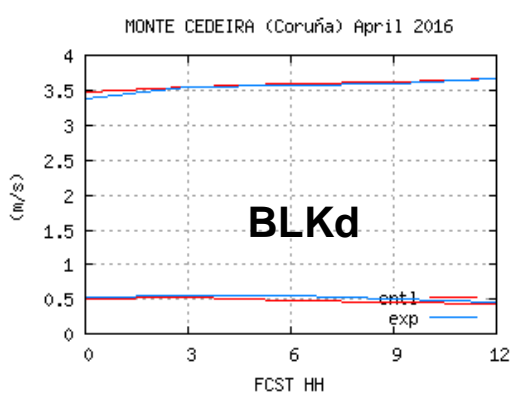
Selection: ALL 469 stations
12h Precipitation Period: 20160401-20160430
Used {06,18} + 12-00

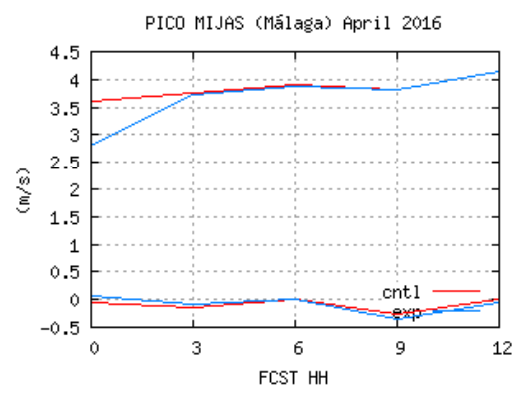
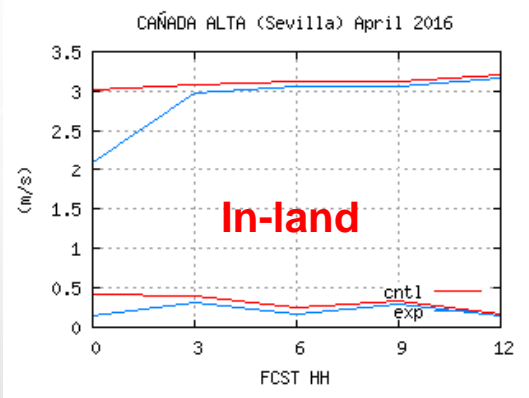
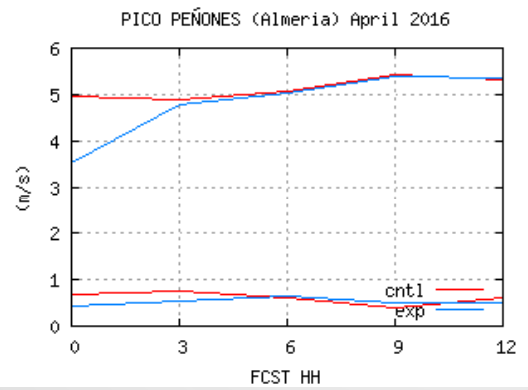
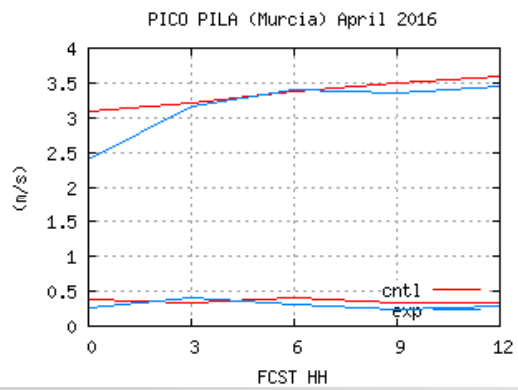
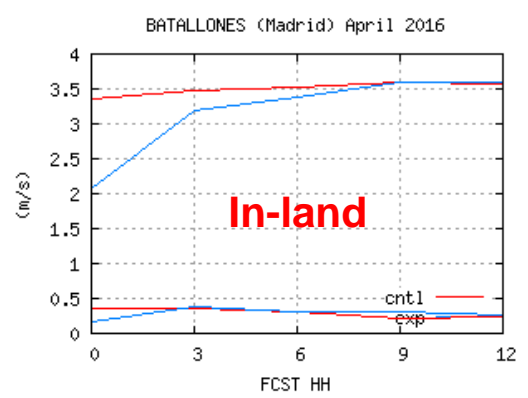
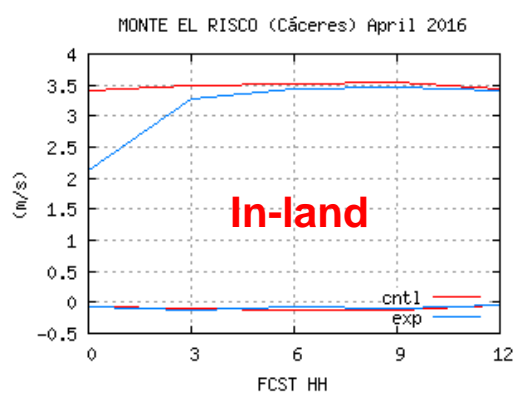


Verification with radar data

$$\text{Error} \equiv \frac{1}{2} * (< (\text{Fcst} - \text{Radar})^2 >^{1/2}_{\text{PPI}=0.5} + < (\text{Fcst} - \text{Radar})^2 >^{1/2}_{\text{PPI}=1.4})$$

1 month (April 2016)



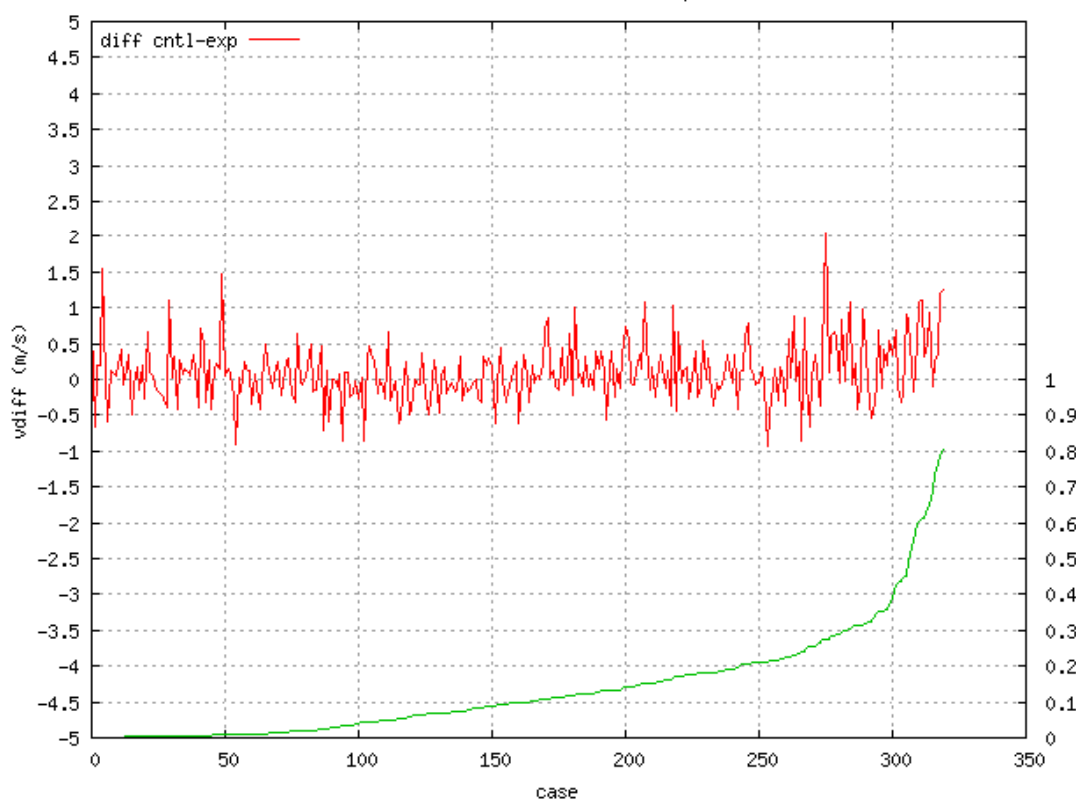


Verification with radar data

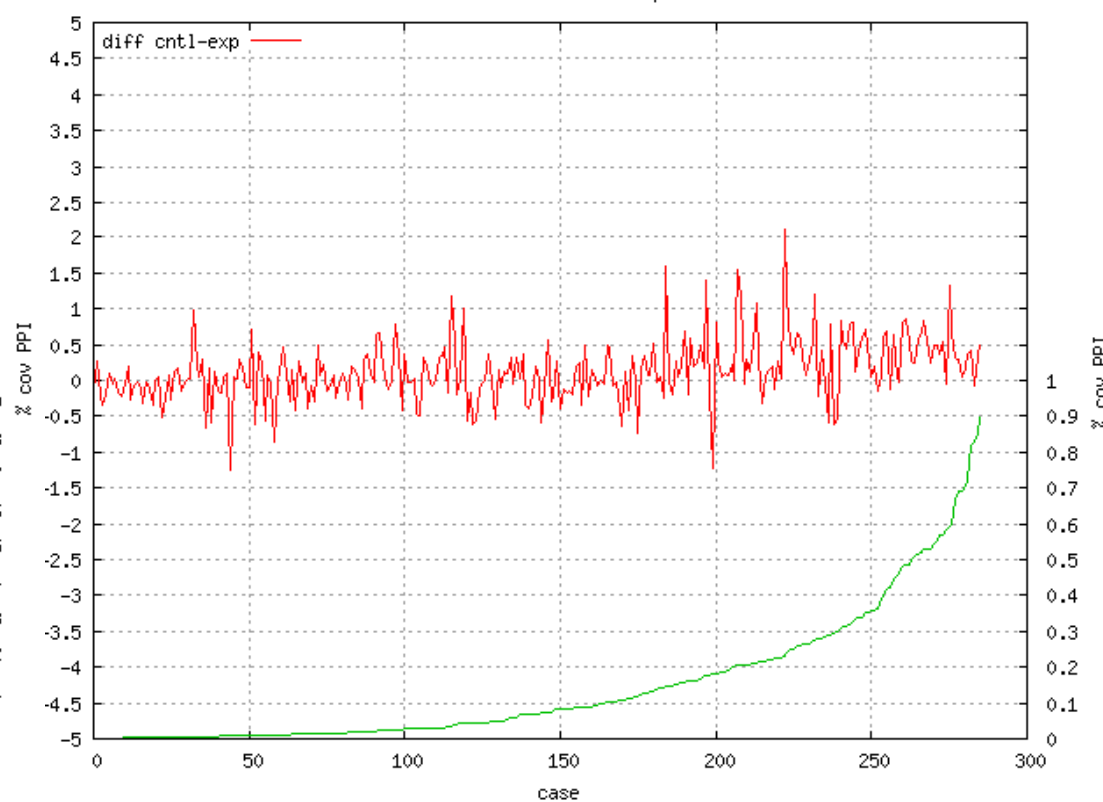
$$\text{Error} \equiv \frac{1}{2} * (\langle (\text{Fcst} - \text{Radar})^2 \rangle_{\text{PPI}=0.5}^{1/2} + \langle (\text{Fcst} - \text{Radar})^2 \rangle_{\text{PPI}=1.4}^{1/2})$$

1 month (April 2016)

RADAR SANSEBASTIAN Forecast +03 April 2016



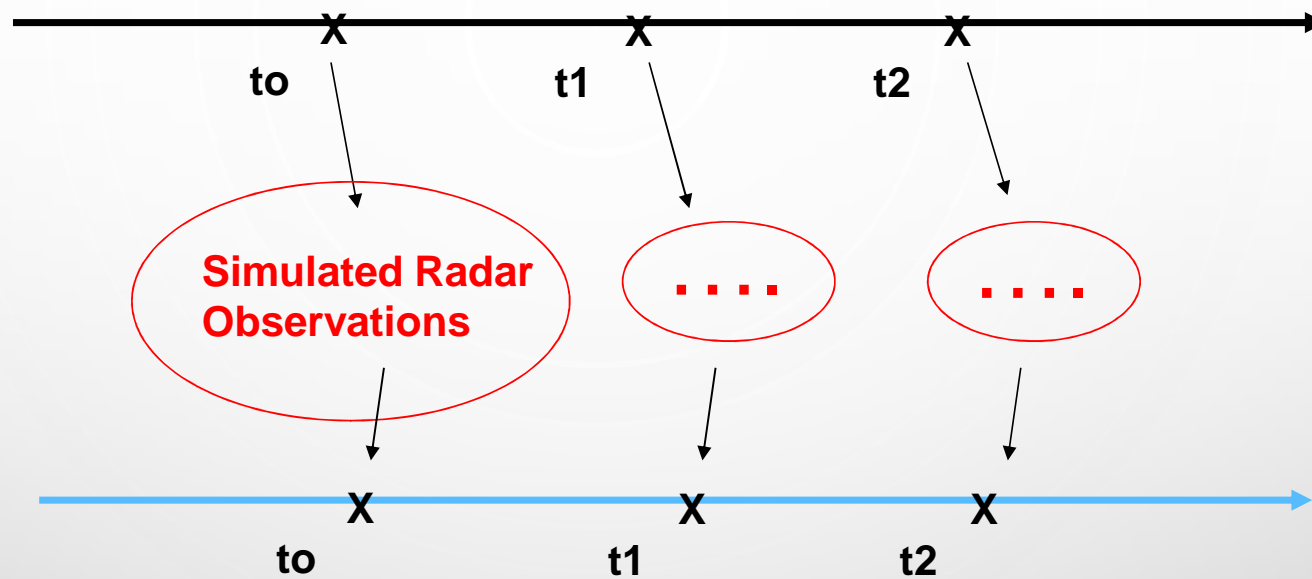
RADAR MADRID Forecast +03 April 2016



Experiments with Simulated Observations offer many advantages:

- Easy access to the validation at all scales
- “Perfect Model” scenario (Models maybe realistic but imperfect)
- Sensitivity analysis to model and/or observations noise
- Freedom to test also hypothetical radar data acquisition schedules (ranges, elevations, number of PPIs,...)

Twin0 (“nature”) : Init + LBC from enda#1



TwinN (“expN”) : Init + LBC from enda#4

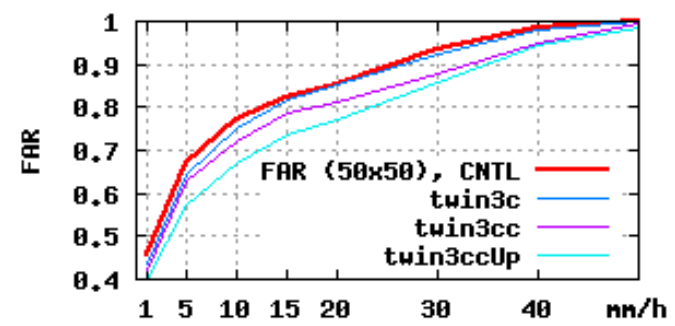
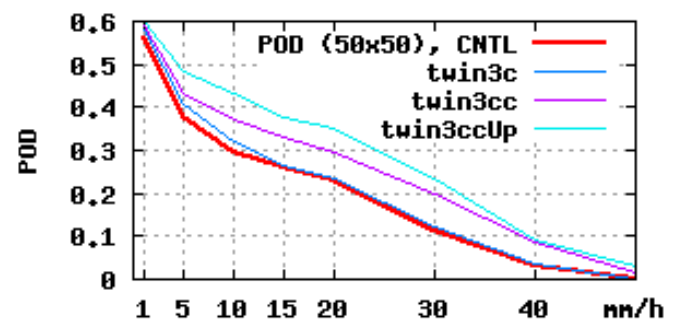
Twin1 (“CNTL”) : Init + LBC from enda#4

Validaton with Simulated Observations : Precipitation Intensity (mm/h) (at grid point level)

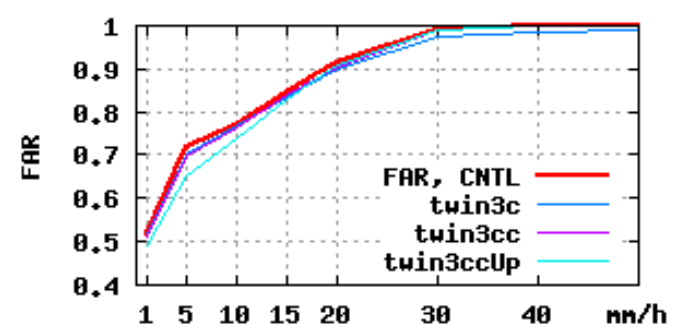
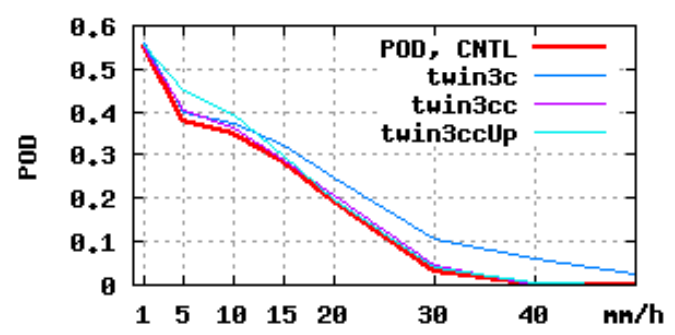
Prob. of Detection

False Alarm Rate

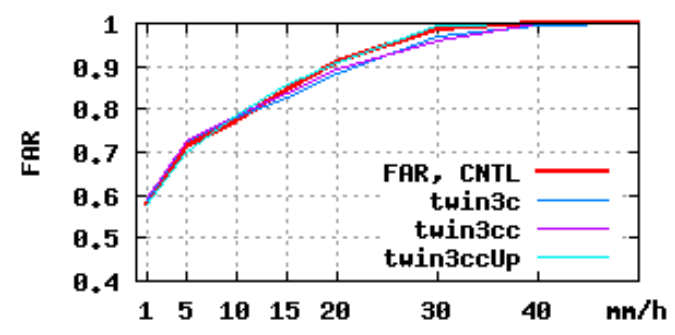
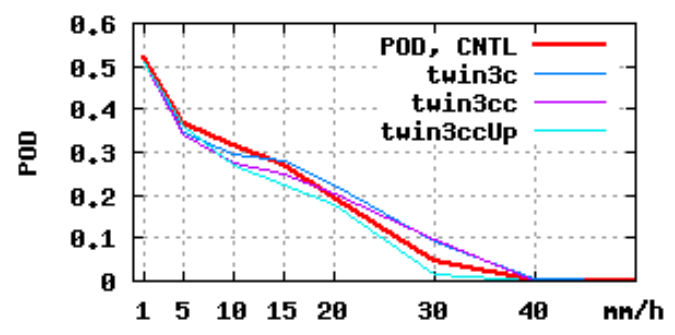
+1 , +3



+4 , +6



+7 , +9



Validaton with Simulated Observations : Precipitation Intensity (mm/h) (at grid point level)

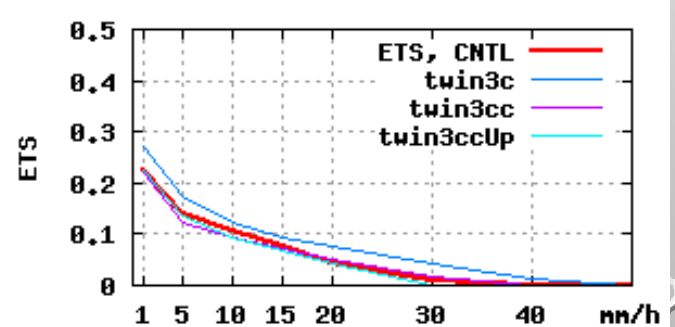
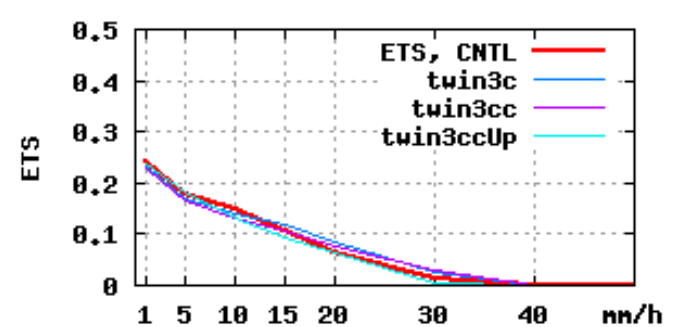
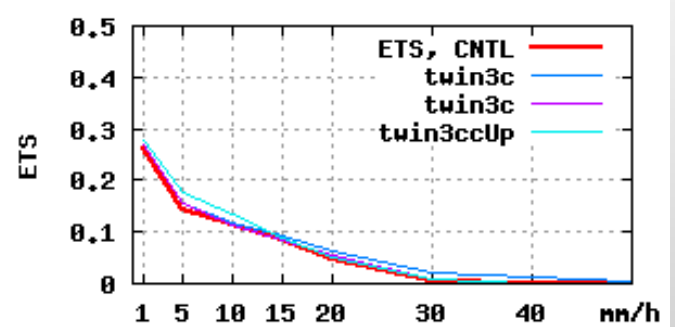
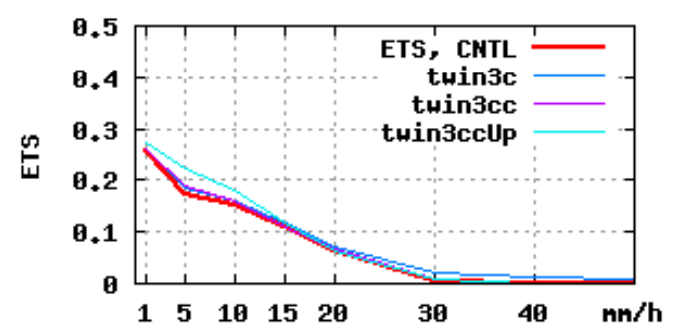
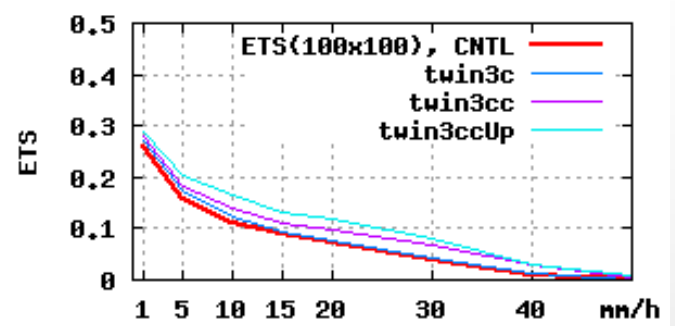
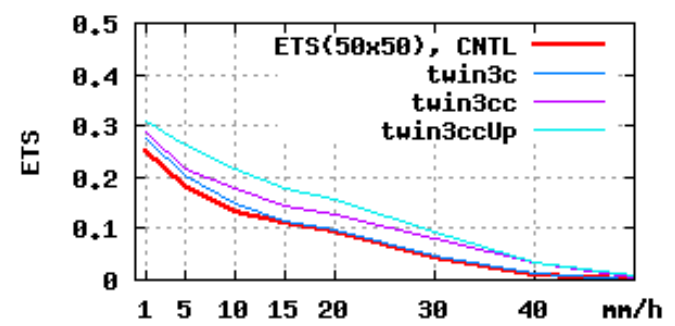
+1 , +3

+4 , +6

+7 , +9

ETS : Small area

ETS : Big area



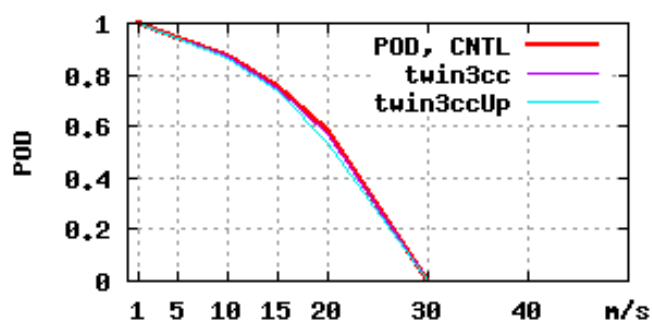
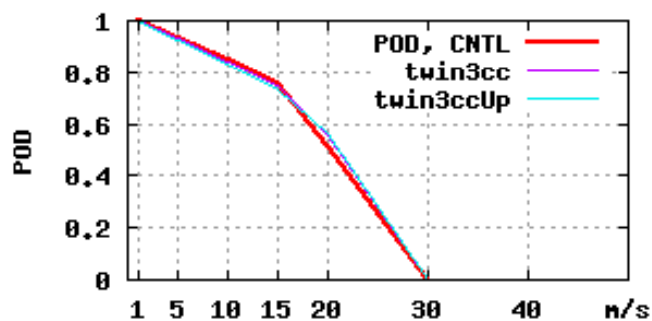
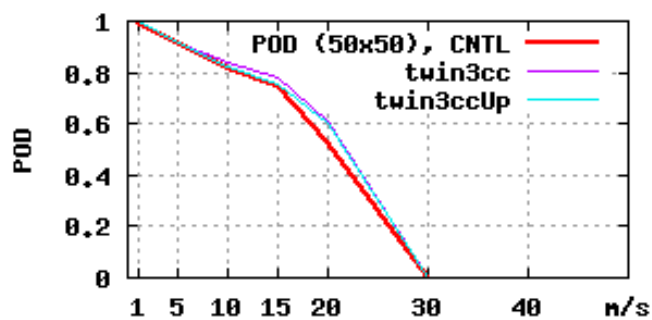
Validaton with Simulated Observations : Wind Gust (m/s) (at grid point level)

+1 , +3

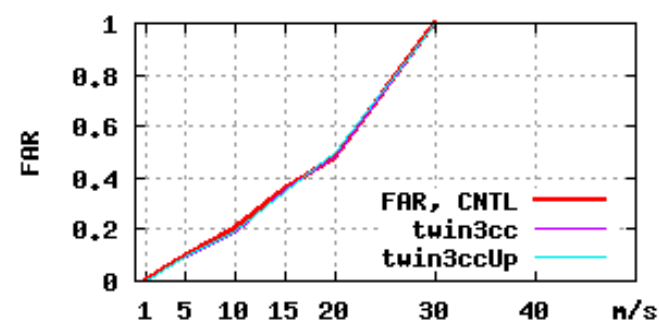
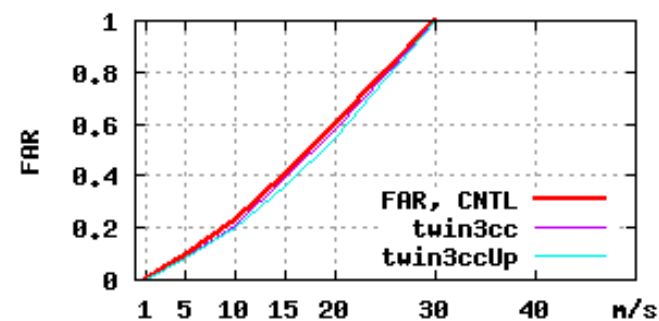
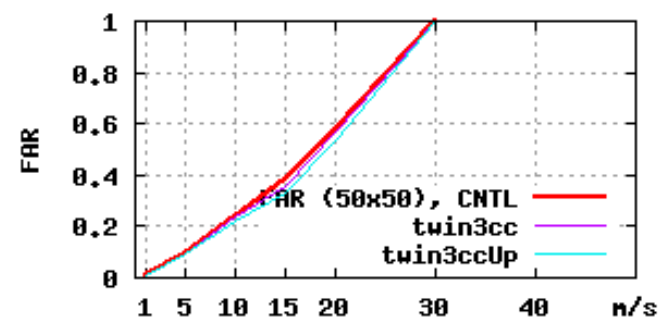
+4 , +6

+7 , +9

Prob. of Detection



False Alarm Rate

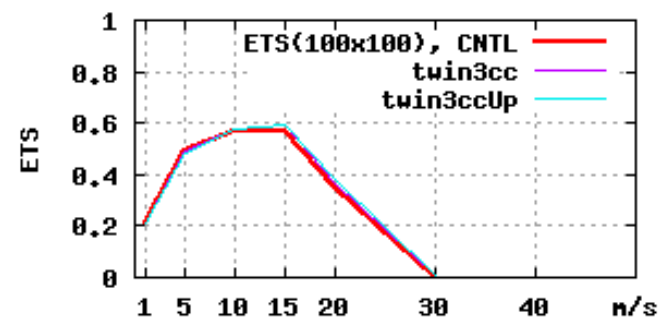
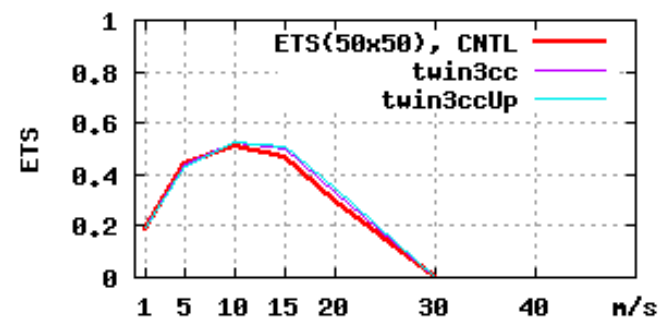


Validaton with Simulated Observations : Wind Gust (m/s) (at grid point level)

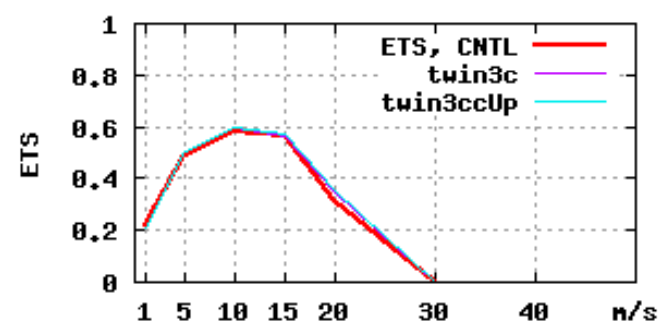
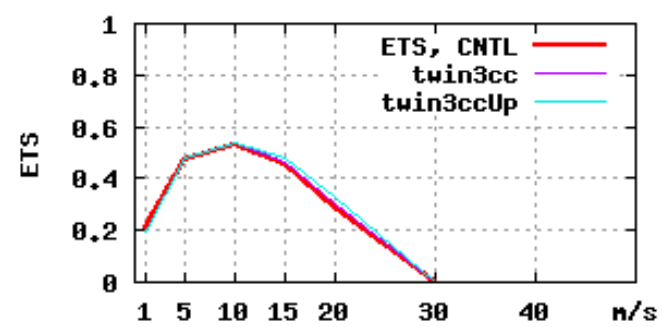
ETS : Small area

ETS : Big area

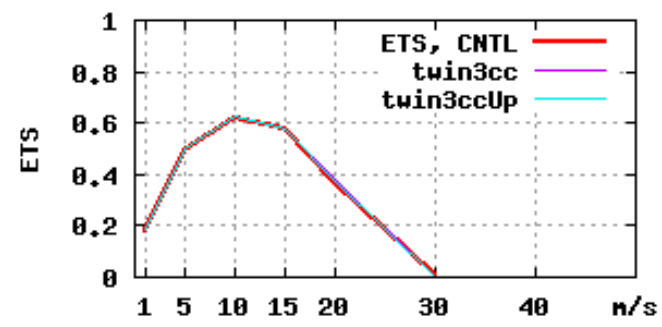
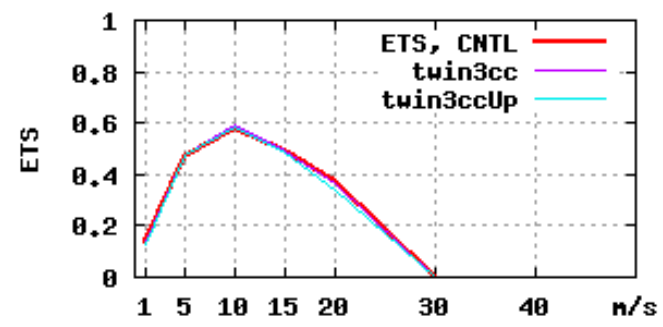
+1 , +3

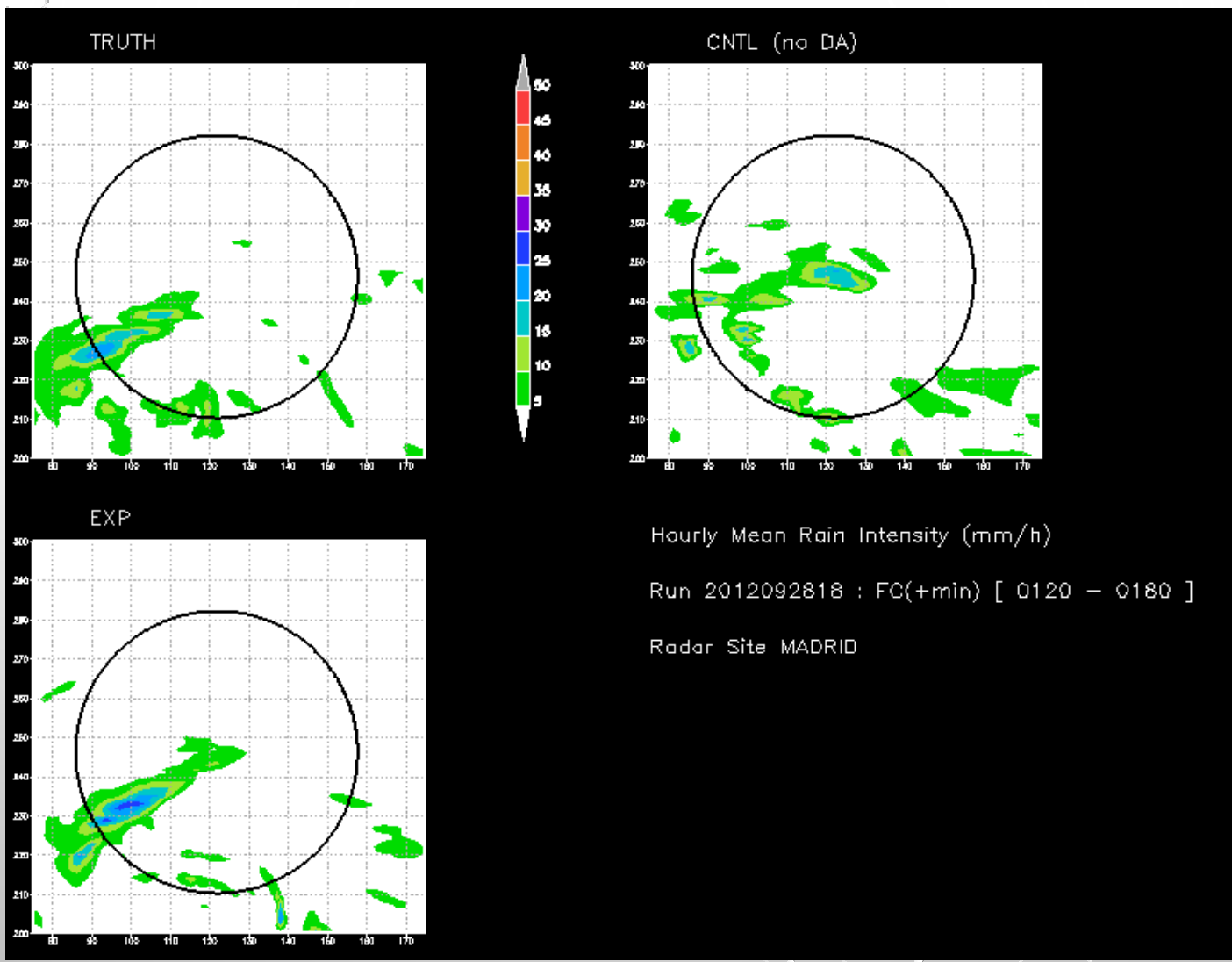


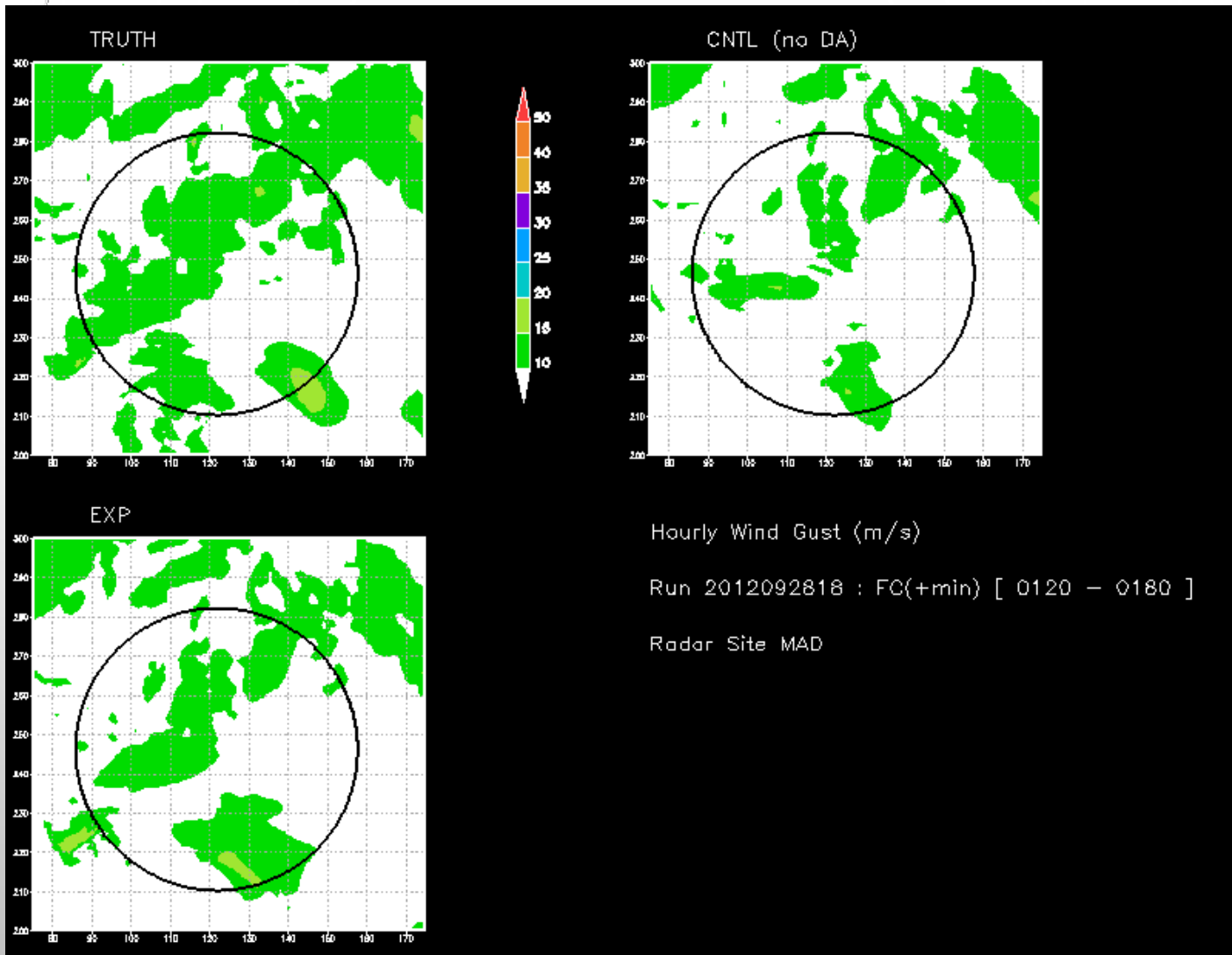
+4 , +6



+7 , +9







- The experiments show that noise filtering and interpolation of the corrections improve the results

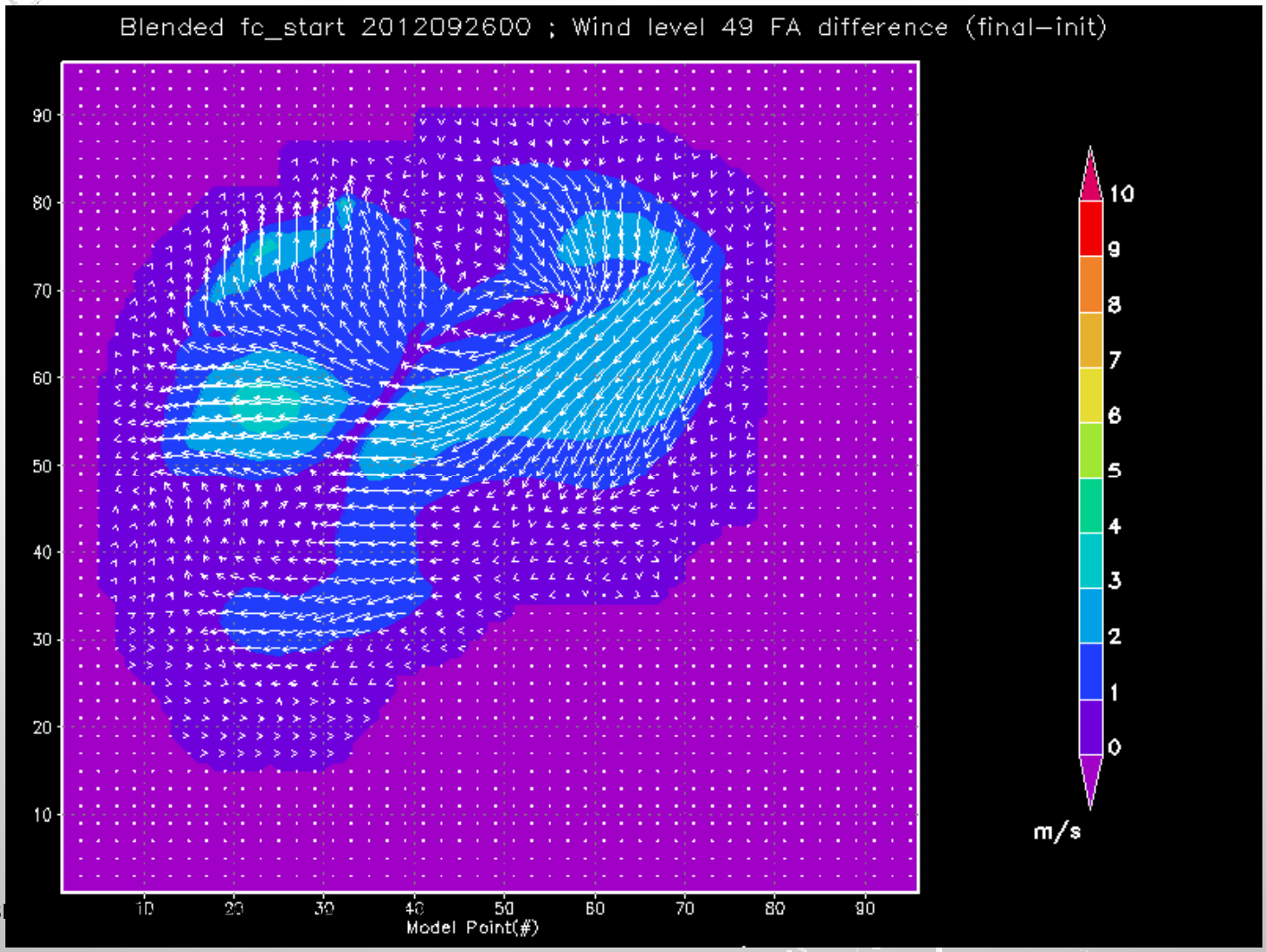
This processing can be carried out using the model error spatial covariances. The rationale behind this lays in the identification of the FA correction with a (model) position error:

$$\varepsilon_b = (\varepsilon_b)_{pos} + (\varepsilon_b)_{other} \approx (\varepsilon_b)_{pos}; \quad \delta FA = -(\varepsilon_b)_{pos} + \varepsilon_{FA} \quad ; \quad \langle \varepsilon_b \varepsilon_{FA} \rangle = 0 \quad (1)$$

This “up-scaling” is implemented as BLUE $\hat{\delta FA}_a := \sum_{\omega \in \Omega} W_{a\omega} \delta FA_\omega$

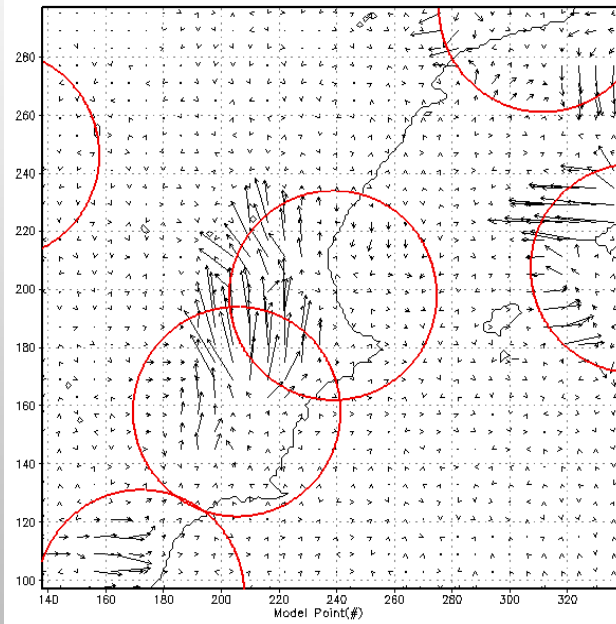
But this problem is solved if the spatial covariances of the δFA random field are known, which under (1) are

$$\langle \delta FA^T \delta FA \rangle \approx \langle \varepsilon_b^T \varepsilon_b \rangle + \langle \varepsilon_{FA}^T \varepsilon_{FA} \rangle \approx \langle \varepsilon_b^T \varepsilon_b \rangle + \begin{pmatrix} \sigma_{FA}^2(1) & \dots & 0 \\ \vdots & \ddots & \vdots \\ 0 & \dots & \sigma_{FA}^2(\Omega) \end{pmatrix}$$

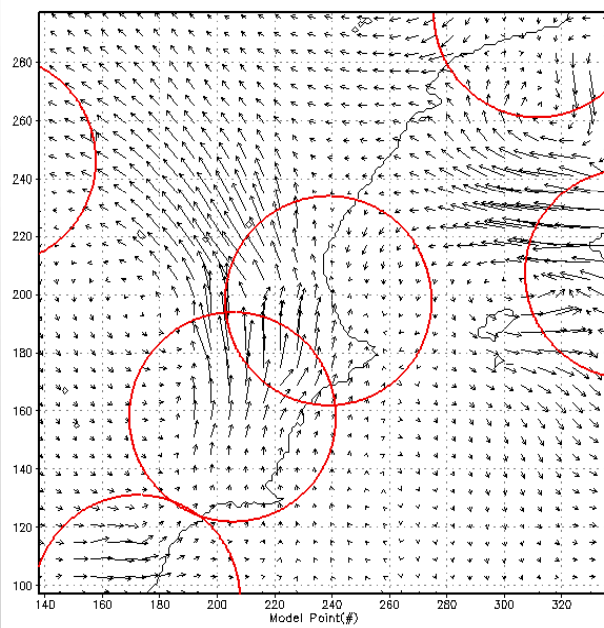


Assimilation of Doppler Wind Radar Data in HARMONIE

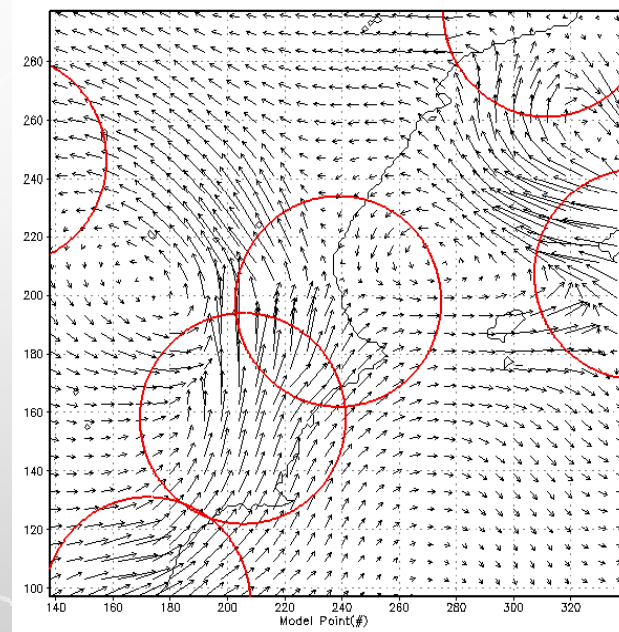
(a)



(b)



(c)



Variational Constraints in DA

Consider the variational constraints encoded in the operator M

$$2J(x^k) = \int_0^{\bar{\xi}} w_o^k \|x^k - x_o^k\|^2 + w_c^k \|Mx^k - x_c^k\|^2$$

Search for a solution in the vicinity of the background

$$x^k = x_b^k + \Delta x^k \quad ; \quad x^k - x_o^k = -d^k + \Delta x^k \quad ; \quad d^k = x_o^k - x_b^k \quad ; \quad Mx^k - x_c^k = M\Delta x^k$$

Weak-constraint formulation $M^+ M \Delta x^k + w^k \Delta x^k = w^k d^k \quad w^k \equiv \frac{w_o^k}{w_c^k}$

Strongly constraint problem

$$M \Delta x = 0 \quad M^+ \lambda + \Delta x = d$$

$$\delta J = \nabla_{\lambda} J \delta \lambda + \nabla_{\Delta x} J \delta \Delta x + \nabla_{\Delta x(0, \bar{\xi})} J \delta \Delta x(0, \bar{\xi}) + \nabla_{\partial \Delta x(0, \bar{\xi})} J \delta(\partial \Delta x(0, \bar{\xi}))$$

Formulation of Balances for ALADIN-NH dynamics (I)

- The GEOGW is closer to available observations than VDPD

- Only rotational invariant scalars. Resting base-state. Flat orography.

$$D - K^2 (T + (\partial + 1)\Psi) = D^\bullet$$

$$K^2 = (kH)^2 (N\Delta t)^2$$

$$N^2 = \frac{g}{H} = \frac{g^2}{RT^*} \quad D = D' \Delta t$$

$$gw - \omega_b^2 ((\partial + 1)T + (\partial + 1)\partial\Psi) = gw^\bullet$$

$$\omega_b^2 = (N\Delta t)^2$$

$$gw = gw' \Delta t / RT^*$$

$$T + \frac{R}{c_v} (D - \partial gw) = T^\bullet$$

$$T = T' / T^*$$

$$\pi_s + N[D] = \pi_s^\bullet$$

$$\pi_s = \pi'_s / \pi_s^*$$

$$\Psi - gw + S[D] = \Psi^\bullet$$

$$\Psi = (\Phi_s + \Phi') / RT^* + \pi' / \pi^*$$

Formulation of Balances for ALADIN-NH dynamics (")

- M and its adjoint M⁺ are reducible to lower and upper triangular forms

$$M = \begin{bmatrix} L & 0 & 0 & 0 & 0 \\ -K^2 \left(1 + \frac{c_p}{c_v} \partial\right) & \left(1 + K^2 \frac{c_p}{c_v}\right) & 0 & 0 & 0 \\ -\frac{R}{c_v} \partial & \frac{R}{c_v} & 1 & 0 & 0 \\ 0 & N[] & 0 & 1 & 0 \\ -1 & S[] & 0 & 0 & 1 \end{bmatrix} \quad M^+ = \begin{bmatrix} L^+ & -K^2 \left(1 - \frac{c_p}{c_v} \partial\right) & \frac{R}{c_v} \partial & 0 & -1 \\ 0 & \left(1 + K^2 \frac{c_p}{c_v}\right) & \frac{R}{c_v} & N^+[] & S^+[] \\ 0 & 0 & 1 & 0 & 0 \\ 0 & 0 & 0 & 1 & 0 \\ 0 & 0 & 0 & 0 & 1 \end{bmatrix}$$

$$S[X] = e^{-\xi} \int_0^{\xi} e^z X \quad S^+[X] = e^{\xi} \int_{\xi}^{\bar{\xi}} e^{-z} X \quad N[X] = e^{-\xi} \int_0^{\bar{\xi}} e^z X \quad N^+[X] = e^{\xi - \bar{\xi}} \int_0^{\bar{\xi}} X$$

$$L[X] = (\partial^2 + \partial - \lambda)X \quad L^+[X] = (\partial^2 - \partial - \lambda)X + BT_L \quad \partial[X] = \partial X \quad \partial^+[X] = -\partial X + BT_\partial$$

Formulation of Balances for ALADIN-NH dynamics (and IIII)

- M+M is also reducible to triangular form and its Greens Function is easy to calculate

$$L^+L[\Delta gw] = F_{gw} + \frac{K^2}{(1+K^2\gamma)}(1-\gamma\partial)F_D - \frac{R}{c_v}\left(\partial + \frac{1}{(1+K^2\gamma)}\right)F_T + \left(1 - \frac{1}{(1+K^2\gamma)}S^+\right)F_\psi + \frac{1}{(1+K^2\gamma)}N^+[F_{\pi_s}\delta]$$

$$L^+L \equiv \lambda^2 - (2\lambda+1)\partial^2 + \partial^4$$

$$-K^2(1+\gamma\partial)\Delta gw + (1+K^2\gamma)\Delta D = \frac{1}{(1+K^2\gamma)}\left(F_D - \frac{R}{c_v}F_T - N^+[F_{\pi_s}\delta] - S^+[F_\psi]\right)$$

$$-\frac{R}{c_v}\partial \Delta gw + \frac{R}{c_v}\Delta D + \Delta T = F_T$$

$$N[\Delta D] + \Delta\pi_s = F_{\pi_s}$$

$$-\Delta gw + S[\Delta D] + \Delta\Psi = F_\psi$$

Variational Constraints and ALADIN 3D-Var Statistical Balance

- It is possible to establish a clear analogy between this theory and the formulation of statistical balances in the ALADIN 3D-Var Algorithm (Derber and Bouttier, 1999)
- The analogy suggests a convenient extension to non-hydrostatic DA, which at the moment we do not have
- A key aspect of this similarity is the de-coupling of (total) wave-numbers in both DA algorithms, although for different reasons in each case
- Two possible implementations of these ideas. The variational one is free of sampling noise and also avoids the artificial splitting between balanced and un-balanced components
- In spite of the similitude, important differences are expected in the results depending on the choice

Variational Constraints and ALADIN 3D-Var Statistical Balance

In the PE model, the SI system involves just three variables (η , T , p_s). The statistical balance formulation for this set reads

$$B = B^{\frac{T}{2}} B^{\frac{1}{2}} \quad B^{\frac{1}{2}} = B_u^{\frac{1}{2}} K^T \quad B_u = \begin{bmatrix} C(\eta) & 0 \\ 0 & C(T, p_s)_u \end{bmatrix} \quad K = \begin{bmatrix} 1 & 0 \\ P & 1 \end{bmatrix} \quad (T, p_s)_b = P\eta$$

with the balance operator P in obvious connection with the (integral) operators τ_r (e.g. $S[\]$) and v_r (e.g. $N[\]$) of the PE SI. The cost function gradient equation :

$$\vec{\nabla} J = B^{-1} \delta x + R^{-1} (\delta x - d) = 0 \quad B_u^{-1} K^{-1} \begin{bmatrix} \eta \\ (T, p_s) \end{bmatrix} + K^T R^{-1} \begin{bmatrix} \eta \\ (T, p_s) \end{bmatrix} = K^T R^{-1} \begin{bmatrix} d_\eta \\ d_{(T, p_s)} \end{bmatrix}$$

Implies the following correspondence with the M+M equation

$$B^{-1} \Leftrightarrow M^+ M \quad M \Leftrightarrow B_u^{-1/2} K^{-1} \quad \eta \Leftrightarrow \Delta g w \quad C_\eta^{-1} \Leftrightarrow C_{gw}^{-1} \Leftrightarrow L^+ L$$

Variational Constraints and ALADIN 3D-Var Statistical Balance

The following balances operator seems then better suited to the SI NH dynamics

$$K_{NH} = \begin{pmatrix} 1 & 0 & 0 & 0 \\ A & 1 & 0 & 0 \\ B & C & 1 & 0 \\ D & E & 0 & 1 \end{pmatrix}$$

$$\eta_b = A \text{ gw}$$

$$(T, p_s)_b = B \text{ gw} + C \eta_u$$

$$\Psi_b = D \text{ gw} + E \eta_u$$

to account for large-scale mass-wind hydrostatic equilibrium, also another plausible candidate is

$$K_{NH} = \begin{pmatrix} 1 & & \dots & 0 \\ 0 & 1 & & \vdots \\ MH & A & 1 & \\ NH & B & C & 1 \\ 0 & D & E & 0 & 1 \end{pmatrix}$$

$$\eta_b = MH\xi + A \text{ gw}$$

$$(T, p_s)_b = NH\xi + B \text{ gw} + C \eta_u$$

$$\Psi_b = D \text{ gw} + E \eta_u$$

Variational Constraints and ALADIN 3D-Var Statistical Balances

- This analysis strongly suggests that balances in NH should be implied from gw and δ and not from ξ alone as in PE
- With this formulation, vertical velocity analysis increments will be produced by K^T_{NH} observations of D, T, p_s and/or Ψ even if vertical velocity obs are not available
- The identification $C_{gw} \Leftrightarrow (L^+L)^{-1}$ provides an analytical model for the co-variance matrix and is in line with the Greens Function as response function to a “unit impulse”
- The Greens Function for the elliptical operators L^+L and L display a clear vertical broadening with larger horizontal scales, in correspondence to the “non-separability” property of the co-variance matrices in the statistical formulation



Grazie tante per la vostra attenzione